DEPARTMENT of INDUSTRIAL CHEMISTRY "TOSO MONTANARI"
SECOND CYCLE DEGREE IN

LOW CARBON TECHNOLOGIES AND SUSTAINABLE CHEMISTRY

CLASSE LM-71

SCIENZE E TECNOLOGIE DELLA CHIMICA INDUSTRIALE

Production of Hybrid Hydroxyapatite-Hollow Pollen Microcapsules for Waste Treatment

Supervisor:
Prof. Silvia Panzavolta

Candidate:
Guliz Erdem

Academic Year 2024-2025

Table of Contents

CHAPTERS

1. Abstract

The main objective of this thesis is to create hollow pollen grains by removing organic components from specific spherical, porous pollen grains. This process involves removing organic matter to leave behind sturdy, hollow structures that can serve a variety of purposes. After the organic content is removed, these hollow pollen shells are filled with synthetic hydroxyapatite (HA), a biologically compatible material widely used in biomedical and engineering fields, particularly in bone and tooth repair. By incorporating HA into hollow pollen shells, we obtain complex materials with a combination of properties useful in various industries, such as environmental science (e.g., wastewater treatment, water improvement) and biomedical applications (e.g., bone tissue regeneration, dental restoration).

This study focuses on analyzing the physicochemical properties of "Millefiori pollen" and also includes the identification of sunflower (Helianthus annuus), Atlas cedar (Cedrus deodara), and other pollen types. These different pollen types exhibit distinct characteristics such as various shapes, porosities, and surface textures, making them ideal candidates for creating hollow shells.

In this thesis study, the aim is to develop functional composite materials using only the natural microstructure of Millefiori pollen grains. These pollen grains, which have a spherical and porous structure, were subjected to chemical processes to remove their internal organic content while preserving the outer exine shell. Among the various methods applied, acid-assisted ether extraction ensured the cleanest hollow structures were obtained while minimizing morphological distortion.

The resulting hollow pollen structures were used as biological templates for the synthesis of hydroxyapatite (HA), a biocompatible inorganic material widely used in both biomedical and environmental applications. The synthesized pollen-HA composites were characterized using analytical techniques such as SEM and EDS, and it was confirmed that HA successfully precipitated into and around the pollen shells.

The adsorption performance of these composites was tested using methylene blue (cationic) and acid red 6 (anionic) dyes as model pollutants. The results obtained demonstrated that the material is effective in dye removal through ion exchange and surface interactions. This study highlights that biomimetic structures derived from pollen offer a promising platform for the development of sustainable hybrid organic–inorganic systems for wastewater treatment.

2. Introduction

Pollen grains function as the male gametophyte structures in seed-bearing plants and are characterized by intricate biochemical and structural features. These microscopic entities are evolutionarily adapted for fertilization and exhibit remarkable resilience against harsh environmental conditions, owing to their layered wall composition and metabolically dynamic cytoplasmic contents.

Owing to their distinct morphology and structural intricacy, pollen grains have been the subject of extensive investigation in both botany and palynology. More recently, interest in these structures has expanded into materials science and engineering. The outermost protective barrier, the sporoderm, is composed of two main layers: the exine and the intine. of particular interest is the exine layer, primarily built from sporopollenin, an exceptionally resilient biopolymer known for its resistance to enzymatic degradation, extreme pH conditions, and elevated temperatures. These characteristics make pollen shells promising candidates as natural microcapsules for chemical and industrial applications (Blackmore et al., 2007; Piffanelli et al., 1998).

Although the detailed molecular architecture of sporopollenin remains incompletely characterized, it is understood to consist of a complex network of aromatic structures, long-chain aliphatics, and extensively cross-linked ester and ether functionalities.
This chemical makeup underpins its exceptional durability. Furthermore, exine surfaces often incorporate flavonoid and carotenoid pigments, contributing to both the coloration and species-specific identification of pollen grains.

The robust outer exine layer, dominated by sporopollenin, plays a central role in the extraordinary stability of pollen grains under diverse environmental stresses such as UV exposure, enzymatic breakdown, and fluctuating pH levels (Domínguez et al., 1999; Piffanelli et al., 1998). This resilience, combined with the biological inertness and ecological safety of the structure, makes it an ideal scaffold for further chemical manipulation.

Because of these traits, pollen shells are increasingly studied as naturally derived microcapsules suitable for biomedical and industrial innovations. For example, their high surface area, functional group diversity, and ability to be chemically modified make them attractive platforms for drug delivery, biosensing, enzyme immobilization, and active ingredient encapsulation (Lee et al., 2013).

Pollen exines also offer reactive functional moieties—such as hydroxyl, carboxyl, and ester groups—that are amenable to further chemical customization. This has enabled their use in environmental applications such as the adsorption of heavy metals and dye pollutants from water, supporting their role in sustainable remediation technologies (Mohan et al., 2020; Luo et al., 2021).

The multifunctional properties of these bio-derived capsules arise not only from their species-dependent morphology but also from their chemically tunable surfaces. A growing body of research highlights the feasibility of employing treated pollen shells in medical and environmental applications (Lee et al., 2019; Luo et al., 2021). In this regard, pollen grains that have undergone de-cytoplasming procedures, preserving only the exine, serve as efficient platforms for chemical loading and material integration.

These hollow pollen structures, due to their high surface-to-volume ratios and biodegradable nature, are particularly suitable for forming hybrid composites. For instance, the incorporation of hydroxyapatite (HA) into these shells results in bi ofunctional materials with both mechanical strength and biocompatibility (Zhao et al., 2020; Wang et al., 2022).

From a taxonomic perspective, Helianthus annuus (sunflower) serves as an ideal candidate for exine modification, thanks to its large grain diameter, spherical shape, and sturdy exine walls. Its spiny surface texture has also been reported to enhance microbial capture, which may benefit environmental use cases (Erdtman, 1969).
Cedrus atlantica (Atlas cedar), while less studied, presents a heteropolar and air-sac (saccate) structure potentially advantageous in directed flow systems. Ambrosia artemisiifolia (wild ragweed), notable for its allergenic pollen, has fine and symmetrical grains well-suited for nanoscale modification. Castanea sativa (chestnut), though underrepresented in current literature, may offer mechanical durability and enhanced loading potential due to its lobed exine architecture.

While prior studies offer valuable insights into these species, the experimental portion of this thesis primarily utilized commercially available Millefiori pollen. Despite limited direct references in the literature, Millefiori pollen demonstrates key features—such as tricolporate apertures, a porous architecture, and a resilient exine—making it a practical model for experimental applications.

2.1. Pollen Types and Structures

First, the general characteristics of Millefiori pollen: These pollen grains, which are mostly tricolporate, monad in structure, and medium in size (26–50 µm), are spherical in shape and exhibit a circular pr ofile in polar projection. Thanks to their porous structure, they can be purified of organic material and oil content using acidic treatments. Advanced techniques such as FTIR, SEM, and XRD were used for analysis.

2.1.1. Sunflower Pollen (Helianthus annuus)

Helianthus annuus pollen grains are monad (single unit) in terms of both biological structure and dispersal. When slightly moistened, they fall within the medium size range of 26–30 µm in diameter. The polar and equatorial axis lengths of these pollen grains are largely the same—corresponding to approximately 26–30 µm in size—and are geometrically quite symmetrical. Morphologically, they are tricolporate (three- apertured) colporate pollen grains. With their isopolar characteristics, they exhibit symmetry at their poles and display a circular, generally spherical form in polar view. Even when dry, the circular silhouette is preserved; a tendency to shrink at the aperture points is observed. The P/E (polar-equatorial dimension ratio) value supports the prolate (elongated) form, and they are more commonly observed in an inclined position under a light microscope. These quantitative and qualitative characteristics provide important data for the taxonomic identification of H. annuus pollen and the understanding of ecological distribution models. First, the general characteristics of Millefiori pollen: These pollen grains, which are mostly tricolporate (three-pored), monad (single-celled) in structure, and of medium size (26–50 µm), have a spherical shape and exhibit a circular pr ofile in polar projection. Due to their porous structure, they can be purified of organic material and oil content through acidic treatments. Advanced techniques such as FTIR, SEM, and XRD were used for analysis.

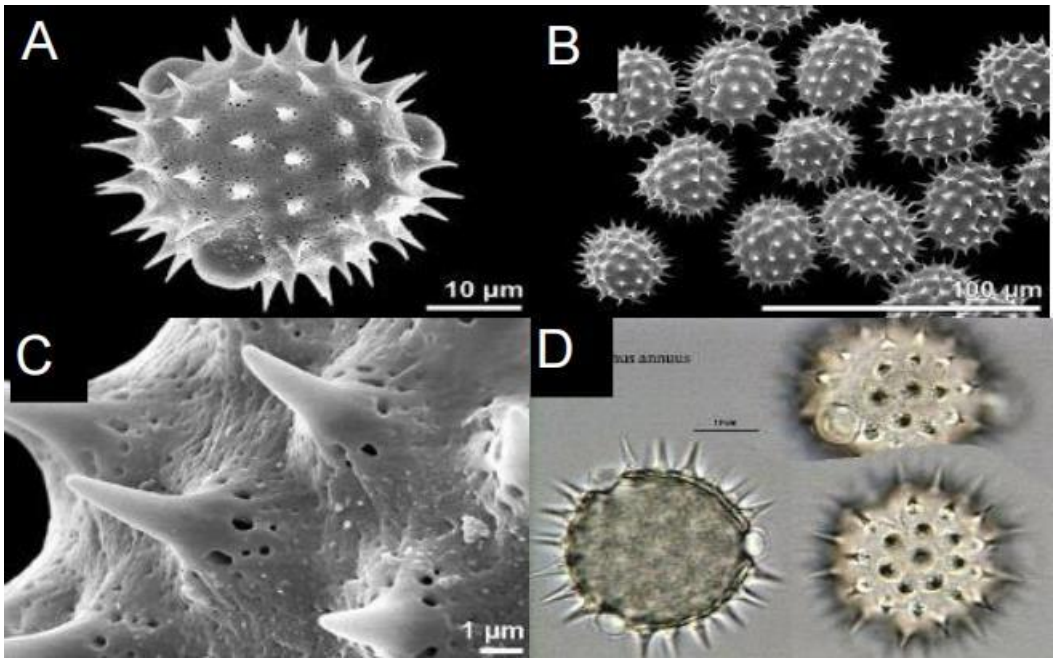

Figure 1. SEM images-Polar view of sunflower pollen structure(A)- Dry pollen grains of sunflower pollen structure(B)-Exine surface of sunflower pollen(C)- Hydrated sunflower pollen (D)

2.1.2. Atlas Cedar (Cedrus Atlantica)

Cedrus atlantica pollen grains are also monad, meaning they occur and spread as individual units. Morphologically, they are defined as “saccate” (sac-like); these sacs enable the pollen grains to gain more lift when carried by the wind. Although moisture measurements are not clearly known, the overall size of the pollen falls into the “large” category (approximately 51–100 µm). One of the prominent features of these pollens is their heteropolarity, meaning there is a structural asymmetry between the poles. This asymmetry is generally related to the specialization of the opening position. In polar view, the pollen has an oval contour, which is important for aerodynamic performance. Its general form can be described as “oblate” (pole-flattened). During examination, a single leptoma-type aperture becomes evident in dried samples, and this aperture has an embedded structure—this structure helps preserve the functional part of the pollen during drying. Although the three-dimensional morphology of the moist or dry state cannot be clearly expressed with existing definitions, the saccate structure and heteropolar asymmetry make Cedrus atlantica pollen easily distinguishable from other species in the Pinaceae family.

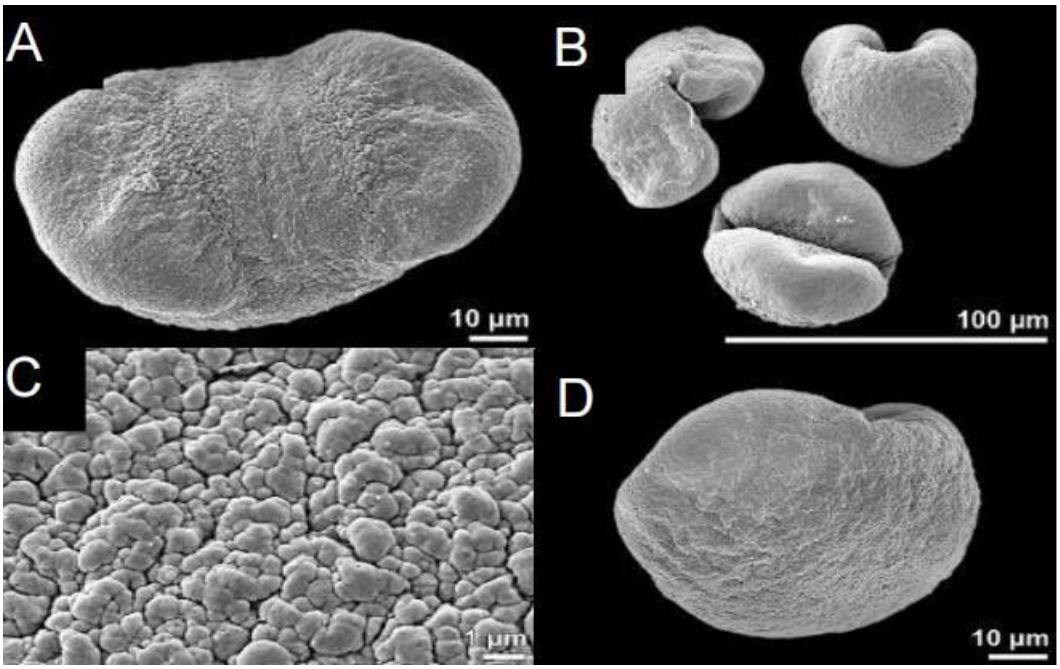

Figure 2. SEM images- Polar view of Atlas Cedar pollen (A)- Dry pollen grains of Atlas Cedar(B)-Exine surface of Adlas Cedar pollen(C)-Equatorial view of Adlas Cedar pollen(D)

2.1.3. Ambrosia(Ambrosia artemisiifolia)

Ambrosia artemisiifolia pollen, commonly known as "ragweed," is found in monad form, i.e., as single units, in terms of structure and distribution. These small pollen grains, typically ranging from 16 to 20 µm in size, facilitate effective transport by wind and increase their allergenic effects with their ability to penetrate deep into the respiratory tract. The similarity in measurements between their polar and equatorial axes indicates that these pollen grains are nearly symmetrical and spherical (spheroidal) in shape. When moist, they appear round in polar projection, but upon drying, the outer wall (exine) contracts, resulting in a more irregular, lobed structure. This is most likely due to mechanical collapse during drying. Structurally, they belong to the tricolporate (three-apertured) colporate pollen class, and these apertures are of the brevikolporus type, with shorter colpi and pores. Due to their isopolar structure, there is no significant difference between the poles. They are typically observed in an

oblique position under a light microscope. When dry, the openings appear sunken inward, which likely serves to protect the opening regions from environmental stresses. These characteristics play a significant role in both the identification of the Ambrosia genus and in ecological and allergenic analysis.

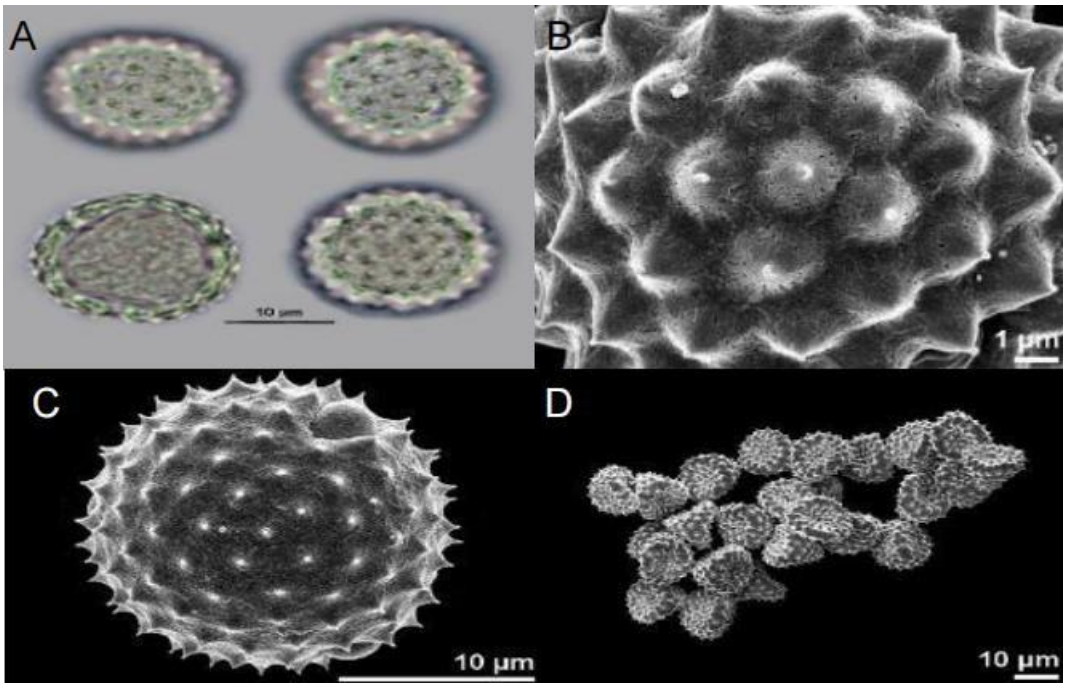

Figure 3. SEM images- Hydrated Pollen Structure of Ambrosia(A)- Exine Surface of Ambrosia Pollen(B)-Polar view of Ambrosia Pollen(C)-Dry Pollen Structure of Ambrosia Pollen(D)

2.1.4. Chestnut (Castanea Sativa)

Chestnut (Castanea sativa) pollen grains, like many wind-pollinated species, are produced and transported in monad form, i.e., as single units. These pollen grains are small in size, typically ranging in diameter from 11 to 15 µm. This small size facilitates effective transport by air currents. Although there is no significant difference between the measurements of the polar and equatorial axes, the polar-equatorial ratio (P/E ratio) reveals that these pollen grains exhibit a form that transitions from spheroidal to prolate (elongated spherical). Their isopolarity indicates structural symmetry between the poles. They are typically observed at an oblique

angle under a light microscope. In their polar view, the pollen grains have a circular structure when moist but adopt a lobed contour when dry. This is likely due to structural folds formed during the drying process. Structurally, these pollen grains belong to the tricolporate (three colporate openings) colporate class. When dry, the openings are generally observed to be sunken inward; this may serve to protect the opening regions from external environmental factors. Castanea sativa pollen grains can be easily identified in palynological analyses based on characteristics such as size, opening configuration, and symmetrical morphology.

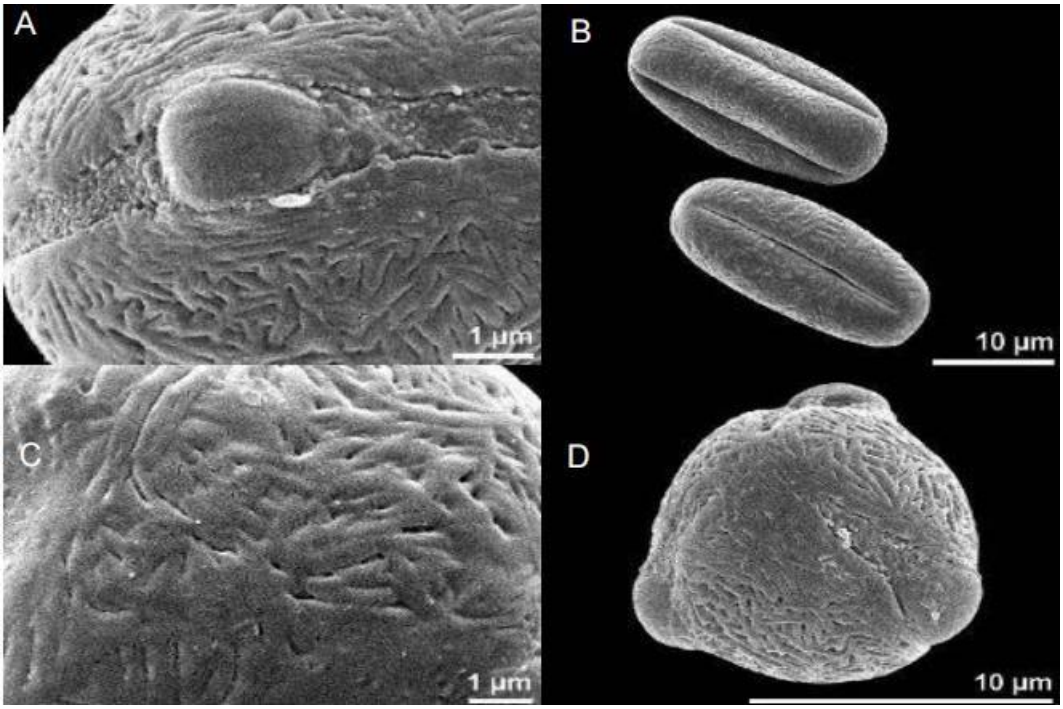

Figure 4. SEM images- Aperture of Chestnut Pollen(A)- Dry Pollen Grains of Chestnut (B)-Exine surface of Chestnut Pollen(C)-Polar view of Chestnut Pollen Grains(D)

2.2 Hydroxyapatite: Structure, Properties, and Applications

Hydroxyapatite (HA) is one of the basic calcium phosphate minerals found in nature that make up the inorganic composition of bones and teeth. Due to its chemical and

crystalline structural similarity to the mineral composition of human skeletal tissue, it has gained great importance in medical fields such as orthopedics and dentistry. This compound, with the chemical formula $Ca_{10}(PO_4)_6(OH)_2$, has a hexagonal crystal system and a molecular weight of approximately 502.31 g/mol. While its pure form is typically white, it can also appear in shades of yellow, green, or gray depending on the presence of trace elements (Dorozhkin, 2010).

In the human body, hydroxyapatite, which constitutes approximately 65–70% of bone mineral content, works in conjunction with collagen to provide mechanical resistance, hardness, and durability to the tissue (Jarcho, 1981). This natural function has inspired the widespread use of both natural and synthetic HA forms in biomedical applications such as bone grafts, dental implants, and orthopedic coatings. Additionally, due to its ion exchange property, HA is also preferred in biotechnological processes such as protein purification and selective adsorption (Elliott, 1994).

One of the most notable aspects of HA is the ease with which ions in its crystalline structure can be replaced by other elements. For example, the addition of magnesium or strontium enhances biological activity while also increasing solubility. On the other hand, the inclusion of fluoride ions reduces solubility and increases chemical stability, leading to the formation of fluorapatite (LeGeros, 2002). These ionic changes directly affect not only HA's thermal and mechanical properties but also its interaction with biological environments. Despite its high biocompatibility, HA is structurally brittle; its flexural strength ranges from 38 to 250 MPa, tensile strength from 38 to 300 MPa, and compressive strength from 100 to 150 MPa. Therefore, when used without reinforcement, there are limitations for high-load-bearing applications (Zhou & Lee, 2011).

HA can be obtained through various methods depending on its intended use. Natural sources include fish bones, animal bones, eggshells, corals, and seashells; these materials are typically calcined at high temperatures to extract HA. In synthetic production, controlled chemical precipitation methods can be used to precisely regulate particle size, morphology, purity, and ion content (Mondal et al., 2019). HA samples derived from waste sources often contain ions such as Mg^{2+}, Na^{+}, CO_3^{2-}, or F^{-} in their structure, which provides an important advantage in enhancing biological activity.

Physicochemically, hydroxyapatite remains stable in neutral and alkaline environments but dissolves at acidic pH values. During this dissolution, calcium and

phosphate ions are released into the environment. This property is particularly important in biomedical applications where HA is biologically controlled to degrade in a controlled manner, supporting tissue remodeling in local acidic environments such as inflammation (Wang et al., 2006). The solubility product constant (Ksp) of hydroxyapatite is extremely low, approximately 2.34×10^{-59} at 25°C, indicating high stability under physiological pH conditions. However, solubility increases significantly when the pH value drops below 6, and this property can also be adjusted by incorporating ions such as carbonate or magnesium into the structure (Kim et al., 2013).

Morphologically, HA particles are typically needle- or rod-shaped, with sizes ranging from nano- to micron-scale. The specific surface area can vary between 20–100 m^2/g depending on the synthesis method. HA derived from waste materials typically exhibits higher porosity and lower crystallinity; while this slightly reduces mechanical strength, it enhances biological activity. High porosity is a highly desirable property in tissue engineering for cell adhesion, nutrient transport, and vascularization (Dorozhkin, 2010).

Beyond biomedical applications, HA also stands out as an effective material in environmental remediation technologies. It acts as a powerful adsorbent in removing substances such as heavy metals (Pb^{2+}, Cd^{2+}, Cu^{2+}) and anionic pollutants (fluoride, phosphate, arsenate) from water. These removal processes occur through mechanisms such as ion exchange (e.g., $Ca^{2+} \leftrightarrow$ metal ions), surface complexation (with phosphate or hydroxyl groups), and the precipitation of insoluble metal phosphates (González et al., 2011). The effectiveness of these interactions is closely related to HA's surface area, porosity, and environmental pH conditions.

As a result, hydroxyapatite stands out as a highly functional material due to its biocompatibility, ion exchange capacity, and adjustable chemical properties. HA obtained from natural biomaterials or laboratory synthesis offers a continuously expanding range of applications in areas such as skeletal tissue regeneration and water purification.

2.2.1. Applications of Pollen in Biomedical Field

Recent studies have shown that pollen grains can be used in the production of composite materials with hydroxyapatite (HA) by evaluating them as natural biomimetic structures. The symmetrical geometry, natural porosity, and biocompatible exine layer of pollen grains make them attractive for biomedical applications, particularly in tissue engineering. These composites have been developed for use in scaffold systems designed specifically for bone regeneration. Pollen structures filled with HA in their inner voids resemble the trabecular (spongy) architecture of bone tissue. This structure has demonstrated high performance in vitro in terms of cell proliferation, adhesion, and osteointegration (Huang et al., 2020; Liu et al., 2021).
Additionally, the bioactive surface formed by integrating HA into the pollen shell enhances interaction with surrounding tissues, thereby accelerating the regenerative process. This makes these composites promising for biodegradable orthopedic coatings and dental implants. Due to their high surface area and ion exchange capacity, these structures have been observed to provide stronger bonding at the bone-implant interface. The interaction between HA's ionic structure (particularly Ca^{2+} and PO_4^{3-} ions) and the hydroxyl and carboxyl groups on the pollen surface creates a microenvironment that supports osteogenic activity (Wang et al., 2019).

2.2.2. Applications of Pollen in Wastewater Treatment

In recent years, pollen grains have attracted attention as an innovative material not only in biomedical applications but also in the field of environmental sustainability. In particular, the use of pollen in wastewater treatment stands out due to the advantages offered by both its natural structure and its processable chemical properties. The hydroxyl (-OH), carboxyl (-COOH), and amine ($-NH_2$) functional groups naturally present on pollen surfaces have the capacity to form strong complex bonds with metal ions and with organic pollutants (Zhou et al., 2022; Huang et al., 2021).

Chemically modified pollen samples—especially variants obtained after alkaline, acidic, or surfactant treatments—show significant increases in surface area and adsorption capacity. This enables the efficient retention of heavy metal ions such as Pb^{2+}, Cd^{2+}, and Zn^{2+}, as well as cationic dyes like methylene blue and rhodamine B

(Liu et al., 2020). The adsorption mechanism is primarily explained by electrostatic interactions, complex formation, and hydrogen bonds.

When these natural adsorbents are combined with hydroxyapatite (HA) to form composites, their ion exchange capabilities are further enhanced. The structural potential of HA to exchange Ca^{2+} ions with metal ions such as Pb^{2+} and Cu^{2+}, along with its ability to form metal phosphate precipitates via phosphate groups, transforms pollen-HA composites into highly effective heavy metal binders (Chen et al., 2021; Mondal et al., 2019). These composites remove contaminants from the environment not only through adsorption but also through multiple mechanisms such as precipitation and ion exchange.

These systems, which have a high specific surface area (20–100 m^2/g) and a microporous structure, maintain their structural stability even under low pH conditions and are effective against a wide range of pollutants. In particular, the increased solubility of hydroxyapatite in acidic environments enables controlled ion release and dynamic pollutant retention. Thus, it is possible to design pH-sensitive, controlled pollutant capture systems (Wang et al., 2006; Kim et al., 2013).

In this way, pollen-based HA composites offer not only an ecologically sustainable alternative, but also an economically viable and recyclable one. Developing wastewater treatment solutions that reduce chemical consumption and comply with green chemistry principles further enhances the value of these materials in environmental applications.

3. Scope and Objective of The Thesis

This thesis aims to develop a novel bio-inorganic composite system by utilizing pollen grains as natural microcapsules for hydroxyapatite (HA) loading. The central objective is to remove internal organic components from pollen grains while preserving their structural integrity, thereby generating hollow shells suitable for functionalization. These hollow pollen grains are then employed as carriers for hydroxyapatite a biocompatible calcium phosphate widely used in medical and environmental applications.

The scope of this work encompasses the optimization of various chemical treatment methods to achieve successful deconstruction of the internal pollen matrix. The study initially evaluates alkaline processing using KOH solutions of different concentrations (1M and 2M), and then acidic tretament performed by phosphoric acid (H_3PO_4).
Additionally, a third strategy will be introduced incorporating ethyl ether pretreatment to defat the pollen surface, followed by H_3PO_4 exposure and subsequent purification via aqueous and organic solvent washes.

Hydroxyapatite (HA) will be synthesized in situ within the internal cavities of pollen granules using a controlled precipitation method involving $Ca(OH)_2$ and dropwise addition of H_3PO_4 . The best ratio between the amount of pollen and HA to produce well coated pollen granules will be investigated. Morphological characterization through scanning electron microscopy of treated pollen, hydroxyapatite and composite materials will be performed.

The research integrates experimental design, chemical processing, and advanced material characterization techniques including FTIR, SEM, and XRD. By combining the inherent porosity and morphology of pollen grains with the ion-exchange and adsorption capabilities of hydroxyapatite, this thesis aims to introduce a novel, sustainable material system designed specifically for environmental applications.
Particular emphasis is placed on the removal of industrial dyes and heavy metal ions from aqueous media, positioning the pollen-HA composite as a promising candidate for use in wastewater treatment and water purification technologies.

4. Materials and Methods

4.1. Materials

Millefiori pollen (commercially obtained)

Potassium hydroxide (KOH, analytical grade, Merck)

Phosphoric acid (H_3PO_4, 85%, commercial grade Merck)

Diethyl ether (Et_2O, pure, Merck)

Calcium hydroxide ($Ca(OH)_2$, solid, Merck)

Distilled water, ethanol, and acetone (for washing and purification)

4.2. Preparation of Hollow Pollen Grains

The initial stage involved the chemical removal of internal organic material from commercially obtained millefiori pollen grains to produce hollow structures. A series of chemical treatments were performed to evaluate the effect of different deconstruction strategies.

4.2.1. Method A: Alkaline Treatment (KOH)

In order to measure how our pollen sample would respond to different concentrations of KOH treatments, two separate syntheses were carried out using 1M and 2M KOH. Before the synthesis process, 0.7 grams of pollen for each synthesis was accurately weighed and mechanically ground into a fine powder for use at 1M and 2M concentrations. The powdered pollen was then treated with 10 mL of 1M and 2M potassium hydroxide (KOH) solutions at 25℃ with continuous stirring at 200 rpm for four hours. After alkali treatment, the resulting suspensions were centrifuged at

10,000 rpm for 10 minutes. The solid residues were then washed with distilled water and centrifuged once more to remove residual reagents. However, after drying overnight at 37°C in an incubator, the initially dark yellow solids turned dark green (Figure 5). The final yields from the 1M and 2M KOH treatments were 0.500 g and 0.646 g, respectively. The recovered solids exhibited a hard, consolidated structure that could no longer be pulverized, indicating significant chemical or physical changes in their morphology and texture due to the harsh alkaline environment.

4.2.2. Method B: Acidic Treatment (H_3PO_4)

As an alternative to alkaline treatment, phosphoric acid (H_3PO_4) was used at different concentrations (1 M and 2 M) to remove organic matter more gently. Again, as in the KOH treatment, changes in the pollen sample at different concentrations were observed by both physical and analysis methods. At the beginning of the treatment, 0.7 grams of pollen sample was weighed to be treated with 1M H_3PO_4 . Similarly, 0.7 grams of pollen sample was used for 2M H_3PO_4 treatment. The weighed pollen samples were treated with 10 mL of 1 M and 10 mL of 2 M phosphoric acid (H_3PO_4) in different containers under the same environmental conditions. The mixtures were continuously stirred at 300 rpm at room temperature for 24 h to ensure complete chemical interaction between the acid and the pollen matrix.

4.2.3. Method C: Ether-Assisted Acidic Treatment (Et_2O)

Based on observations, a combined three-step approach was implemented to preserve pollen morphology while enhancing pore accessibility:

Defatting: Pollen samples were incubated in diethyl ether overnight to remove lipophilic surface components. For this process, smaller amounts than those mentioned in the article (Yang Y. et al 2024) were used (1/8 ratio). Instead of the 50

grams of pollen sample mentioned in the article, 6.25 grams of pollen sample were weighed and incubated with 25 mL of ethyl ether at room temperature overnight.

Acidic Deconstruction: The samples were treated with 2 M phosphoric acid for 8 hours at room temperature under continuous agitation (300 rpm). Instead of using 50 grams of pollen as in previous protocols, 6.25 grams of pollen sample were treated with 50 mL of 2 M phosphoric acid (H_3PO_4) and stirred at 37 °C, 300 rpm for 8 hours. Since the original research article did not specify the exact volume or concentration of H_3PO_4 used, the initial trial was conducted with 50 mL as a preliminary estimation, subject to recalculation based on further optimization.

Purification: The resulting suspension was sequentially washed with hot distilled water, acetone, and 2 M hydrochloric acid (HCl). It was then centrifuged at 10,000 rpm for 10 minutes, and the recovered solids were subsequently dried overnight in an incubator set to 37 °C.

4.3. Synthesis of Hydroxapatite

Three different hydroxyapatite production methods were tried.

4.3.1. Method A: Wet-Chemical Precipitation Using $Ca(OH)_2$ and H_3PO_4

In this method, the synthesis procedure was adapted from the study titled “Synthesis of nanocrystalline hydroxyapatite from $Ca(OH)_2$ and H_3PO_4 assisted by ultrasonic irradiation” (Shah et al., 2004), which employs a conventional wet-chemical precipitation approach for hydroxyapatite (HA) formation.

$$10\ Ca(OH)_2 + 6\ H_3PO_4 \rightarrow Ca_{10}(PO_4)_6(OH)_2 + 18\ H_2O$$

50mL, 0.5 M calcium hydroxide [$Ca(OH)_2$] solution was maintained at 37 °C under constant stirring at 200 rpm, while a 50 mL, 0.03 M phosphoric acid (H_3PO_4) solution was added dropwise over a controlled period to initiate the reaction.

Upon completion of the addition, the resulting mixture was centrifuged at high speed, washed to remove residual ions, and dried at 37 °C to obtain the final HA product.

4.3.2. Method B: HEPES-Buffered Calcium Phosphate Precipitation

In this approach for calcium phosphate (CaP) synthesis, more stringent control over temperature and pH was required compared to Method A. To facilitate the formation of hydroxyapatite, two precursor solutions were employed. Solution A consisted of 5 mM sodium phosphate dodecahydrate ($Na_3PO_4 \cdot 12H_2O$) and 36 mM sodium bicarbonate ($NaHCO_3$), both prepared in 40 mM HEPES buffer at pH 7.38. Solution B was composed of 5 mM calcium chloride dihydrate ($CaCl_2 \cdot 2H_2O$), also prepared in the same HEPES-buffered system. Each solution (50 mL) was equilibrated independently at 37 °C for two hours before being combined under continuous stirring. The resulting mixture was maintained at 37 °C for an additional six hours to enable controlled CaP precipitation.

Throughout the mixing process, the pH was carefully regulated and stabilized at 7.74 by incremental addition of hydrochloric acid (HCl). This procedure is consistent with HEPES-buffered precipitation protocols widely adopted in calcium phosphate transfection techniques (Kingston et al., 2001). The mechanistic pathway involves the initial formation of ion-paired complexes (Ca^{2+}/PO_4^{3-}), minor pH fluctuations within the buffered medium, and gradual nucleation favoring hydroxyapatite crystallization over competing phases—all under conditions that closely mimic physiological environments (Kingston et al., 2001; Cheang et al., n.d.)

4.3.3. Method C: Wet-Chemical Precipitation Using $(NH_4)_2HPO_4$) and $Ca(NO_3)_2$

Under continuous stirring, 50 mL of 0.65 M dibasic ammonium phosphate ((NH4)2HPO4) were added dropwise to 50 mL of 1.08 M calcium nitrate tetrahydrate (Ca(NO3)2 . 4H2O) via a dropping funnel over a period of approximately 30 min. Both precursor solutions were pre-adjusted to pH ≈ 10 using concentrated ammonia and kept at 37 °C. After the addition was completed, the mixture was stirred for additional five hours under constant temperature and pH conditions. The resulting precipitate was then collected by centrifugation (10,000 rpm, 10 min), washed three times with distilled water, and dried at 37 °C overnight. 4.761 grams of Hydroxyapatite were obtained.

4.4 In-Situ Synthesis of Hydroxyapatite Within Pollen Shells

4.4.1 In-Situ Synthesis of Hydroxyapatite Within Pollen Shells By Using Method A For HA

The hollow pollen grains obtained via Method C were employed as microreactors for the precipitation of hydroxyapatite. For this method, 0.5 M $Ca(OH)_2$ and 0.03 M H_3PO_4 solutions were used. 0.270 grams of hollow exine capsules produced using Method C were used. For the 0.5 M $Ca(OH)_2$ solution, 0.377 g of $Ca(OH)_2$ were weighed and dissolved in 50 mL of distilled water using a magnetic stirrer. For the 0.03 M H_3PO_4 solution, 0.2 mL of 85% commercial acid were taken and added to 50 mL of distilled water. 50 mL of $Ca(OH)_2$ solution were poured into a 2-3 neck flask in a water bath, 0.270 grams of empty exine capsule sample were added to this solution, and the phosphoric acid solution was slowly dripped into the $Ca(OH)_2$ and pollen-containing solution at 37 degrees for approximately 50-60 minutes at 200 rpm. After the reaction was complete, the sample was centrifuged at 10,000 rpm for 10 minutes, then filtered and washed twice, filtered again, and

left in a desiccator at 37 degrees for one night. The formation of HA in the hybrid materials was assessed by XRD and SEM.

A further synthesis was performed by varying the ratio pollen/HA. The empty exine capsules were kept at the same amount (0.270 g), and the volumes of $Ca(OH)_2$ and H_3PO_4 were reduced by a 1:5 ratio, using 10 mL of 0.5 M $Ca(OH)_2$ and 10 mL of 0.03 M H_3PO_4 solutions to repeat the process.

4.4.2 In-Situ Synthesis of Hydroxyapatite Within Pollen Shells By Using Method C for HA

Following this production method, an in-situ study was conducted to create a complex product consisting of hydroxyapatite-empty pollen capsules. As in method A, empty exine capsules (0.2 g) were added to a flask containing 50 mL of 1.08 M ($Ca(NO_3)_2 \cdot 4H_2O$) solution, and 50 mL of 0.65 M phosphate solution was slowly added at 37 °C and 300 rpm. The resulting precipitate was then collected by centrifugation (10,000 rpm, 10 min), three times washed with distilled water, and dried overnight at 37 °C.

In a further synthesis, the method was repeated under the same conditions to produce a hybrid product by using a 1:5 ratio and doubling the amount of empty exine capsules (0.4 g). The method was also repeated for hydroxyapatite production alone, maintaining the 1:5 ratio for yield analysis and calculation purposes.

4.5. Evaluation of Removal Efficiency of Composite Materials

4.5.1. Removal of Dyes

In this study, two types of dyes were used to test how well they stick to surfaces: Acid Red 6 (AR6) and Methylene Blue (MB). These chosen dyes have different chemical structures and behave differently when dissolved in water. This allows us to test how

well the materials can remove various types of contaminants. Acid Red 6 (AR6) is a type of dye that is used to color things. Its full name is Sodium 3-[[4-(benzoylethylamino)-2-methylphenyl]azo]-4-hydroxynaphthalene-1-sulphonate, but that's a complicated way to say it. It is a special kind of dye called an anionic azo dye. The molecule has one or more azo groups (-N=N-) in its structure, which is what gives it color. AR6 is a man-made color used a lot in making clothes, leather goods, and paper. It has a sulfonate ($-SO_3^-$) group in its structure, which makes it have a negative charge when mixed with water. This property helps it make strong connections with positively charged materials through electric attraction. Also, because it has aromatic rings, it can stick to surfaces by using special types of bonds called π-π interactions and hydrogen bonds. Methylene Blue (MB) is a type of dye. Its full name is a long chemical name, but basically, it's a dye that carries a positive charge. This dye, which comes from phenothiazine, is commonly used for coloring in biology experiments, light-based treatments, and fighting germs. The positive charge of MB in water helps it stick to materials that have negative charges on their surface. The dimethylamino groups ($–N(CH_3)_2$) in its chemical structure can connect with surfaces that have a lot of electrons because they can give electrons away. Also, MB helps with how things stick to surfaces through interactions called π-π stacking because it has a ring-like structure. The different charges of these two dyes have allowed us to compare the surface properties of the materials that hold them. For example, the carboxyl and hydroxyl groups found on surfaces from pollen are likely to push away negatively charged dyes and strongly attract positively charged dyes. On the other hand, materials like hydroxyapatite, which can exchange ions, can attract negatively charged dyes because they have calcium ions on their surface. This is very helpful for removing pollutants in two ways. Tests on how substances stick to surfaces have shown that both the attraction between charged particles and how well the surface fits (like the size of holes and the area) are important for getting rid of dyes. Also, the color removal rates measured using UV-vis spectra for these dyes have shown that the adsorbent materials work well.

Materials:

Raw pollen

Pollen treated by method C

HA powders obtained by method A

Composite pollen-HA (pollen obtained by method C + HA obtained by method A)

will be evaluated.

Calibration curves of each dye were obtained by solubilizing the powders in distilled water. The curves are displayed in the results and discussion section.

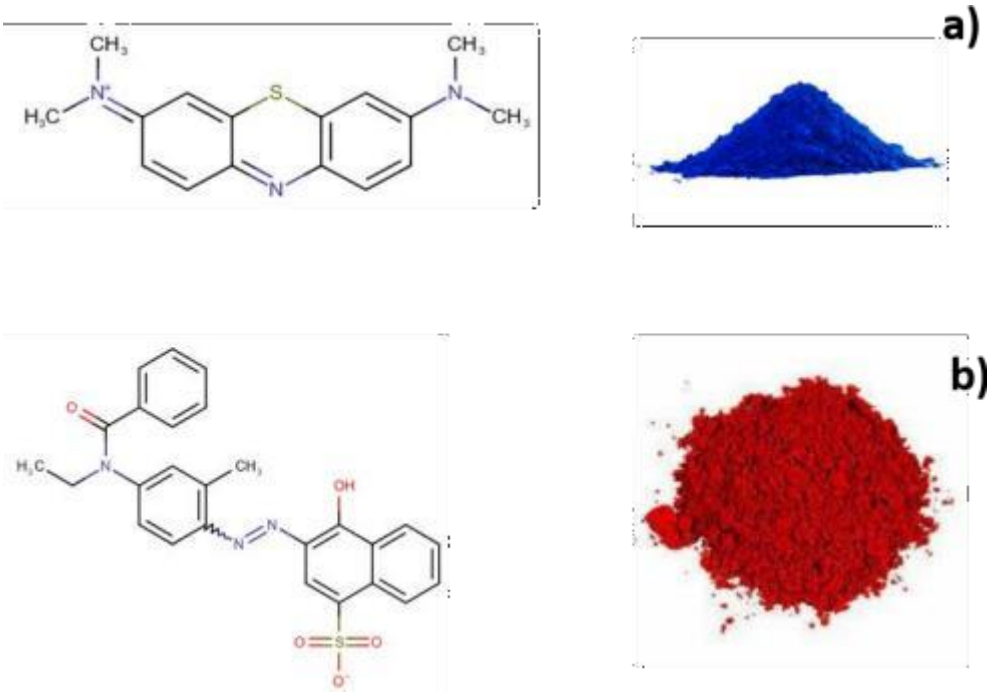

Figure 5. Molecular formula and optical picture of a) methylene blue; b) Acid red 6

Equation 1) and 2) were used to calculate the removal efficiency (RE %) and the adsorption capacity (Qe)

$$RE = \frac{(C0-Ce)}{C0} * 100$$

eq 1

$$Qe = \frac{(C0-Ce)*V}{m} \quad \text{eq 2}$$

Where:

C0 = starting concentration of dye (mg/L);
Ce = equilibrium concentration of dye after selected time of treatment (mg/L); V = volume (L);
m = mass (g) of adsorbent

Removal efficiency of acid red 6 dye

A 50 ppm acid red dye solution was prepared by diluting a 500 ppm stock solution freshly prepared. Next, 20 mg of the adsorbent were added to a beaker containing 25 mL of the 50-ppm dye solution. The mixture was treated for 2 hours at a temperature of 26–30°C under continuous stirring at 300 rpm. After treatment, the solution was centrifuged at 10,000 rpm for 4 minutes to separate the supernatant, which was then analyzed using UV-visible spectroscopy.

Removal efficiency of methylene blu dye

The adsorption of methylene blue was examined by treating 25 mL of a 50 ppm methylene blue solution with 25 mg of adsorbents for 2 hours at a temperature range of 26–30 ºC and a stirring speed of 300 rpm. After treatment, the solution was centrifuged at 10,000 rpm for 4 minutes to separate the supernatant, which was then analyzed using UV-Visible spectroscopy.

4.6. Characterization Techniques

To assess the morphological and structural changes during processing, and to confirm HA formation and distribution, the following characterization methods were employed:

Scanning electron microscopy: a Zeiss Leo 15-30 Field Emission electron microscope was used. Samples were mounted on aluminum stubs and coated with gold before observation;

- Infrared spectrophotometry: a Thermo Scientific Smart Performer FTIR-ATR spectrophotometer was used. Spectra were acquired in ATR mode directly on the powder (100 scans; 4 cm-1 resolution);
- X-ray diffractometry of powders: a PANalytical X'Pert PRO diffractometer was used. Diffractograms were collected in the range 5°-60°/2 theta, using K α copper radiation (40 mA, 40KV) and an acquisition time of 5s per step.
- UV-Vis spectroscopy: an Agilent Cary 60 UV-Vis spectrophotometer was used: spectra were acquired in the 800-400 nm range.

5. BCA Protein Test of Exine Pollen Grains

The prepared empty exine capsule sample was subjected to a protein test to evaluate the protein content and the effectiveness of the treatments performed. The sample obtained after applying method C to completely extract the protein content from the exine capsule was compared with the untreated pollen sample. For this purpose, the Bicinchoninic Acid (BCA) Protein Assay method described in the article " Sporopollenin Capsules as Biomimetic Templates for the Synthesis of Hydroxyapatite and β-TCP (De Mori, A., 2024)" was applied. Due to the low protein content of the treated pollen samples, the solutions were used directly, while the untreated pollen solution samples were diluted separately once and twice for calibration due to their high protein content.

Materials:

-NaCl

-KCl

-Na_2HPO_4

-KH_2PO_4

-Distilled water

Preparation of 50 mL PBS (Phosphate Buffer Saline) solution:

-0.4 g of NaCl
-0.01 g KCl
-0.181 g Na_2HPO_4
-0.01225 g KH_2PO_4 measured and completed up to 50 mL with distilled water, then well mixed under room teperature and 200 rpm till every chemical dissolved.

To extract proteins from raw pollen and treated pollen (which obtained by Method C,) 25 mg of each sample were taken and mixed in 6 mL PBS at 25 degrees for 4 hours. Then, after mixing, each sample centrifugated for 5 minute under 2000 rpm and room temperature. After centrifugation, liquid parts was ready to use in protein test.

A total of 5 different samples were prepared:

1) Blank solution containing only PBS and BCA (2 mL of BCA completed it up to 5 mL with PBS)

2) Treated pollen sample 1 mL solution + 2 mL BCA + 2 mL PBS

3) Treated pollen sample 2 mL solution + 2 mL BCA + 1 mL PBS

4) Untreated pollen sample (1 mL + 9 mL PBS) 1 mL was taken from the main solution, dissolved in 2 mL BCA, and 2 mL PBS was added.

5) Untreated pollen sample (1 mL + 9 mL PBS) 1 mL was taken from the main solution, 9 mL PBS was added, and 1 mL of this solution was taken and 2 mL BCA and 2 mL PBS were added.

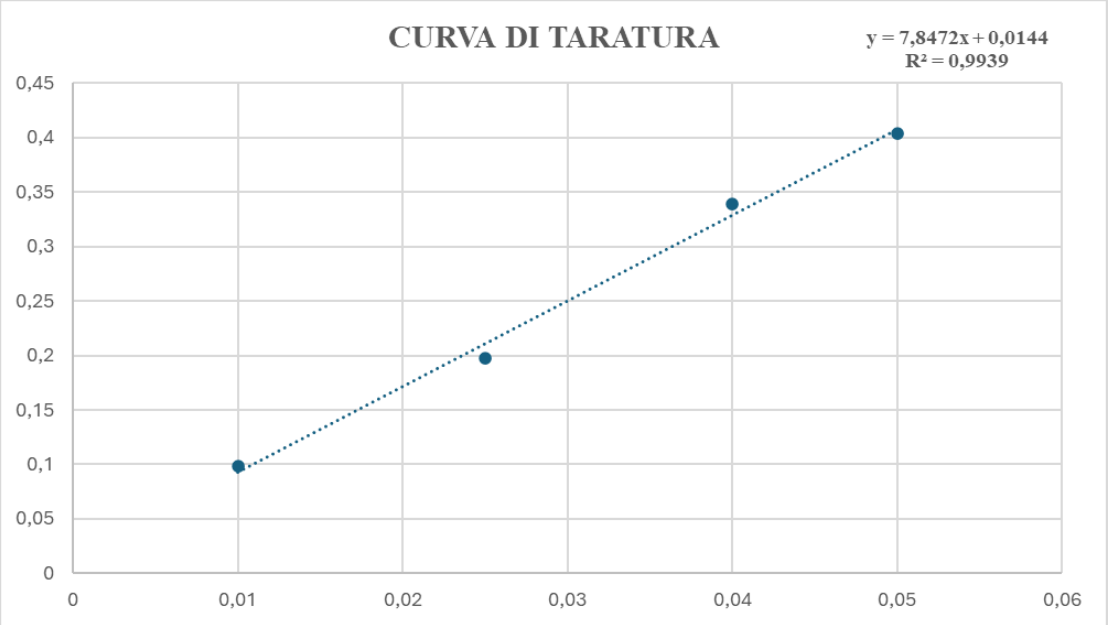

Figure 6. Calibration curve for Bicinchoninic Acid (BCA) Protein Test

Untreated pollen: 12 mg of proteins/25 mg of starting material
Treated pollen: 4,86 mg of proteins/25 mg of starting materail. The treatment performed removed 60% of the total proteins.

These results show a similar success rate when compared to the data reported by De Mori et al. (2024). As a result of the chemical treatments applied in De Mori's study, protein removal in sporopollenin capsules varied between 50-70%, and this showed that protein extraction could be achieved while preserving the capsule structure. In this context, the 60% removal rate obtained confirms the effectiveness of the applied protocol (Method C).

6. Results and Discussions

Due of seasonal issues, the cost and difficult access of selected type of pollens, this study was carried on with “Millefiori” pollen sample, bought at a local grocery. The pollen aggregated granules (Figure 7), have different colors.

Figure 7. Digital image of the pollen aggregated granules " Millefiori" used in this study.

At the SEM, the pollen granules showed a spheroidal shape, with dimensions in the range 10-40 microns (Figure 8A), quite similar to the shape of pollen obtained from Euphorbia Dendiriodes (Figure 8B).

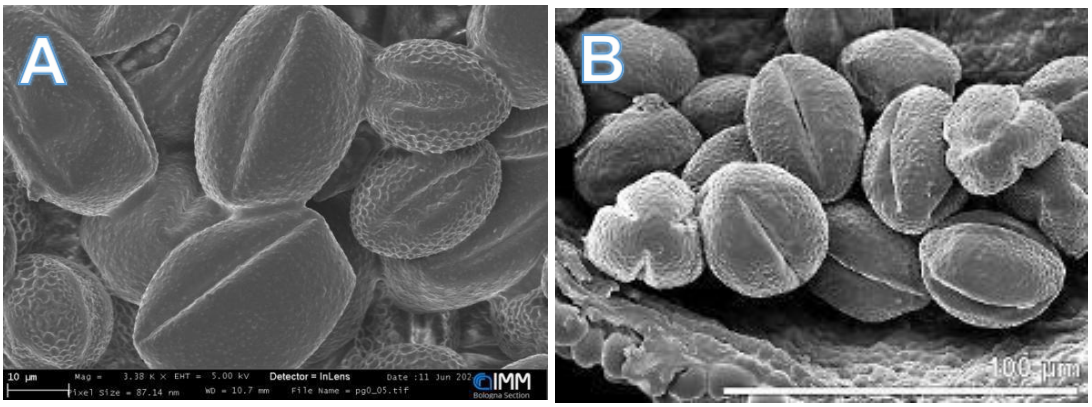

Figure 8. A)Millefiori pollen grains and B)Euphorbia Dendiriodes

Many methods have been described in the literature for producing hollow pollen grains. Depending on the pollen structure, basic treatment, acid treatment, and acetolysis can be considered as basic treatments. In this thesis three different methods were tested to remove organic matter from pollen shells.

Initially, the alkaline Method A approach was used, in which potassium hydroxide (KOH) was applied to treat pollen grains under high pH conditions. This process, which used different KOH concentrations (1M and 2M), damaged the delicate structure of the pollen grains, and a significant portion of the organic particles could not be completely removed (Figure 9). Upon examining the SEM images, it was observed that the pollen samples, which were reduced to powder at the beginning of the process, were completely deformed, and the process was unsuccessful. When we repeated the same process without grinding the pollen grains into powder, it was again observed that the exine capsule form could not be preserved and the pollen grains were not resistant to the alkaline process. Additionally, the fact that a hard solid sample that could not be ground into powder was obtained at the end of each process eliminated the possibility of the exine capsules forming a complex product with hydroxyapatite, leading us to proceed to the next method, the acidic process.

However, SEM observations revealed significant structural damage and deformation, leading to a departure from the original globular morphology. Consequently, this method was discontinued due to excessive degradation of the pollen architecture.

Therefore, a literature review was conducted, and as a result, the phosphoric acid method was used because it is one of the reactants for HA production. In this way, an attempt was made to obtain a method with a high impurity rate using the chemicals we already use to create complex products.

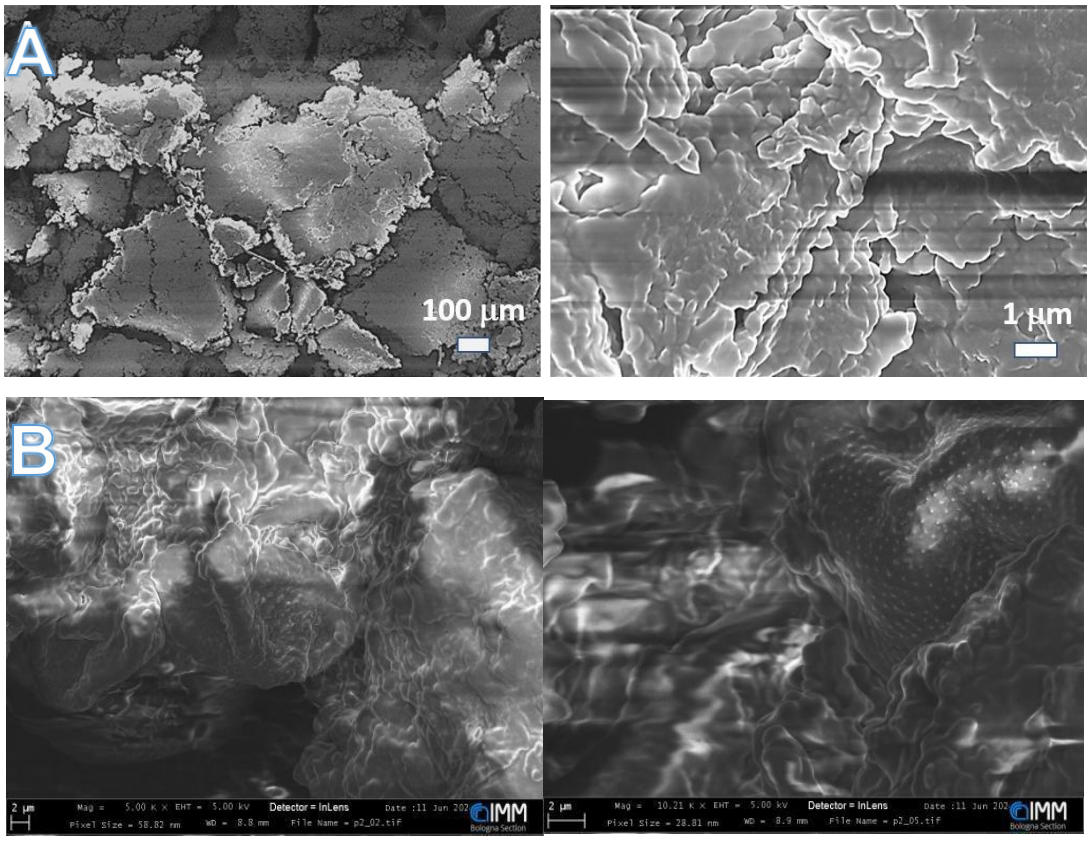

Figure 9. SEM images of Millefiori pollen under 1M of KOH treatment(A) and Millefiori pollen under 2M of KOH treatment(B)

Figure 10. Millefiori pollen after treatment of 1M KOH(A) and Millefiori pollen after treatment of 2M KOH(B)

As a result of the process carried out using method B, pollen treated with 1M H_3PO_4 yielded a lighter yellow color compared to KOH treatment. Additionally, orange spots were observed on the surface of the solution obtained with 2M H_3PO_4 (Figure 11B). These orange spots were thought to be organic particles inside the exin capsules, and it was determined that the removal of organic particles was more successful as the molarity increased during the acidic treatment.

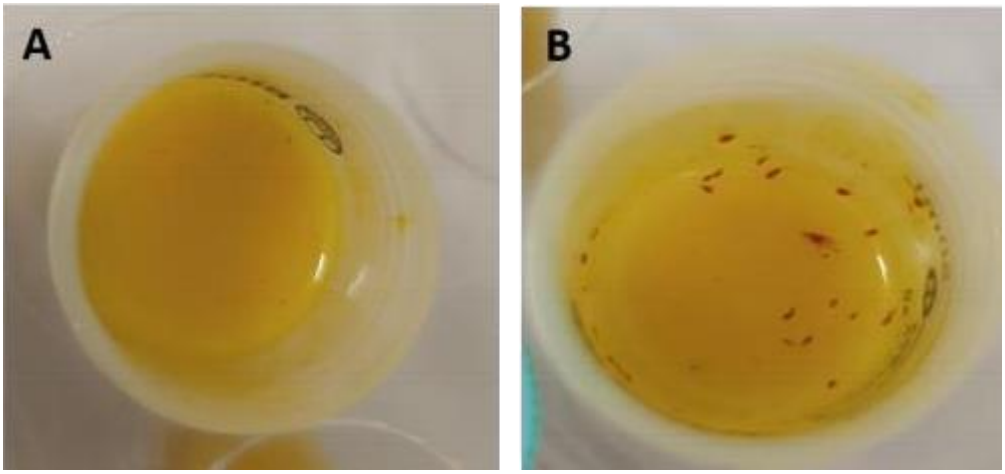

Figure 11. Millefiori pollen after: A) 1M H_3PO_4 treatment; and B) after 2M H_3PO_4 treatment

Following the treatment with phosphoric acid, SEM images revealed that the spherical structure of the exin capsules remained intact but was insufficient for the removal of organic particles (Figure 12).

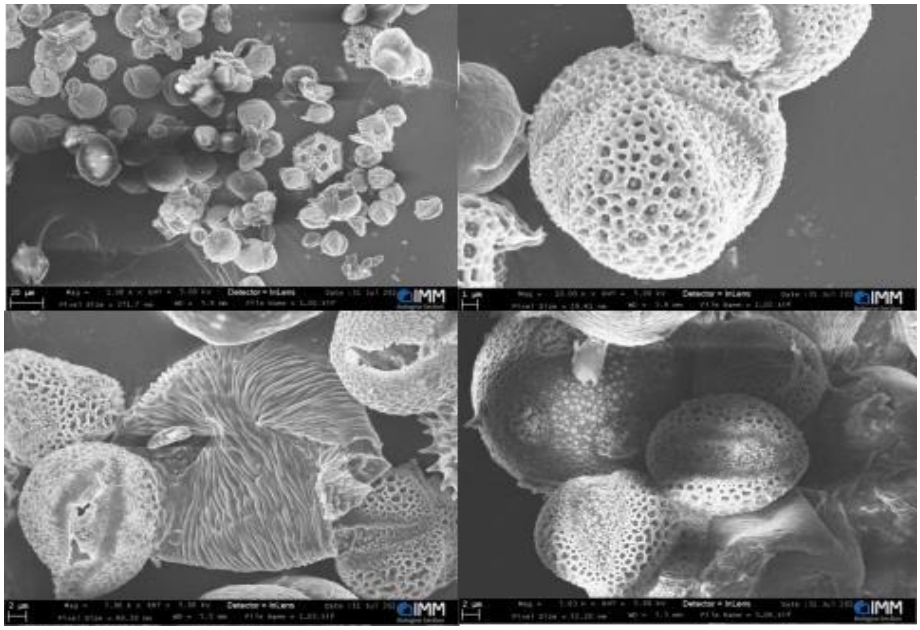

Figure 12. SEM images after 2M H_3PO_4 treatment.

At the same time, a color similar to that of the HSEC granules obtained using the method mentioned in the article “Sunflower pollen-derived microcapsules adsorb light and bacteria for enhanced antimicrobial photothermal therapy”(Yang Y. et al 2024) was obtained.

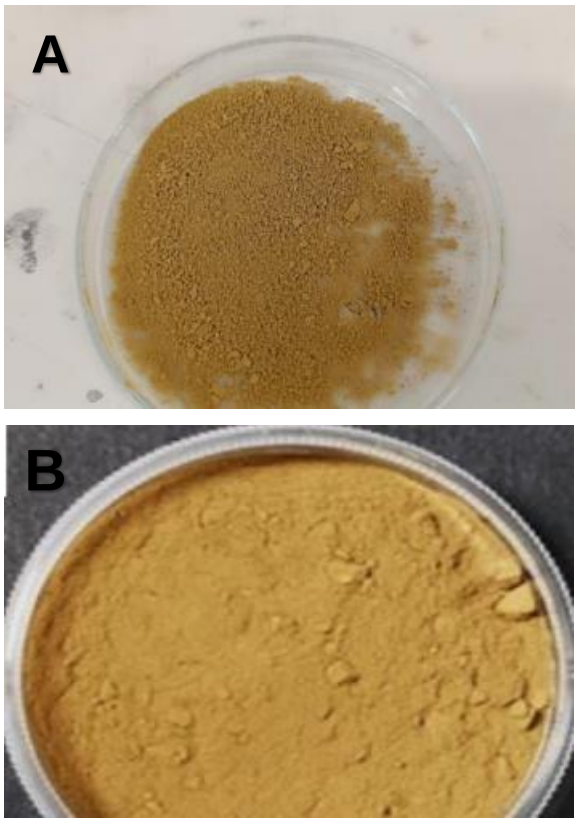

Figure 13. Millefiori pollen after 2M H_3PO_4 treatment(A) and HSEC granules(B)

Instead of the hard, non-powderizable solid sample obtained using Method A (alkaline treatment), a structure that could be more easily powderized was obtained using Method B (acidic treatment). However, upon examining the SEM images, although the pores of the exin capsules were slightly wider than those of the untreated sample, the capsules were not completely free of organic particles. Therefore, based on the research conducted, it was decided to proceed to Method C, as it was believed that the ether-acid process would yield better results (Figure 14).

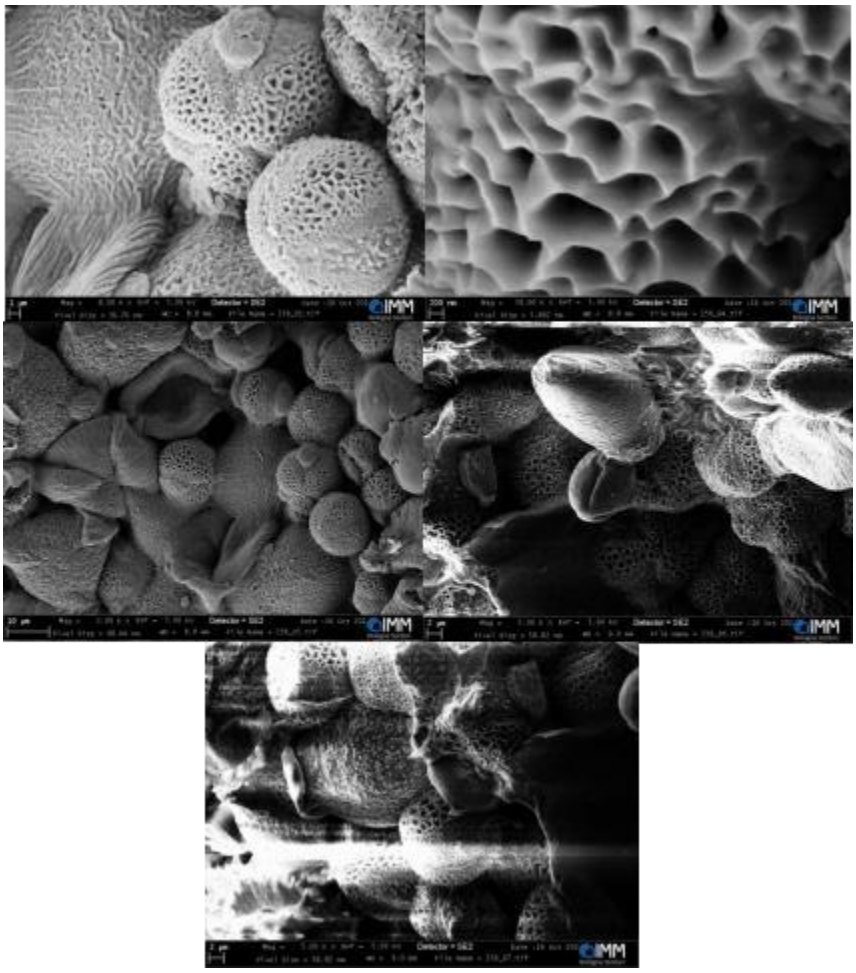

Figure 14. SEM images of Millefiori pollen after Method C treatment

The C method, described in the paper of "Sunflower pollen-derived microcapsules adsorb light and bacteria for enhanced antimicrobial photothermal therapy" includes several steps (defatting, acidic deconstruction, and purification) (Yang Y. et al 2024). Although the type of pollen they used was more resistant, they were successful in achieving their goal of creating empty exine capsules. In the defatting step, after incubating the pollen granules with ethyl ether overnight, it was observed that the pores of the pollen capsules became more open than with the KOH method and that there were no impurities (Figure 15).

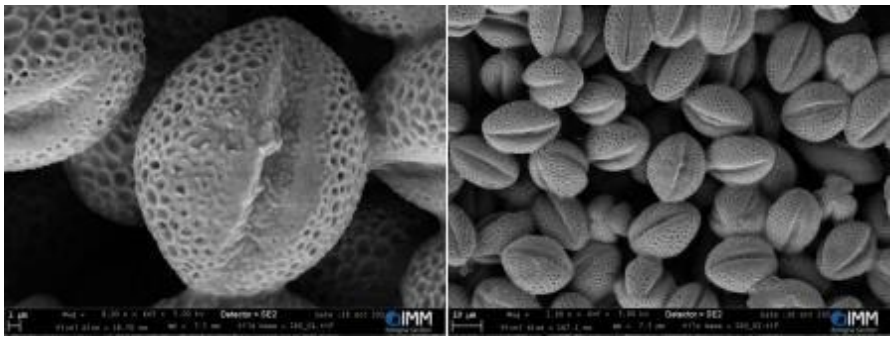

Figure 15. SEM images of Millefiori pollen after ethyl ether incubation

As a result of the Acidic Deconstruction and Purification processes, SEM images showed that the exine capsules were completely free of organic particles, the pores were fully opened, and some completely empty capsules had collapsed (Figure 14). This purification process, which began with 6.25 grams of pollen, resulted in the production of 1.778 grams of empty exine capsules. The observation of only exine capsules, along with the removal of organic particles and impurities, confirmed the success of this pre-treatment process through SEM images.

The Ether-Assisted Acidic Treatment (Method C) successfully removed all organic particles, resulting in intact, empty pollen shells. The empty pollen shells were then filled with hydroxyapatite synthesized in the laboratory using Method A (4.4.2 In-Situ Synthesis of Hdyroxyapatite within Pollen Shells). The presence of HA was confirmed by Xray powder diffraction (Figure 20) and also SEM images showed successful HA formation inside the pollen shells, with external crystallization observed in some cases due to excessive precursor volume or concentration (Figure 17). These observations provided information for further optimization aimed at maximizing intragranular filling while minimizing external deposition. After discussions with the supervisor and calculations were completed in light of this information, the same procedure was repeated using lower amounts of $Ca(OH)_2$ and H_3PO_4 . Empty exine capsules were kept in the same amount (0.270 g) and the volumes of $Ca(OH)_2$ and H_3PO_4 were reduced in a ratio of 1:5 using 10 mL of 0.5 M $Ca(OH)_2$ and 10 mL of 0.03 M H_3PO_4 solutions and the process was repeated. As a result of the process, it was determined that empty exine capsules could be successfully filled with hydroxyapatite, but the external deposition was reduced (shape unknown). In the first application, 0.420 g of hydroxyapatite-filled exine capsules were obtained from 0.270 g of pollen sample treated with 50 mL of $Ca(OH)_2$

and 50 mL of H_3PO_4 solutions; 0.217 g of complex product was obtained from 0.270 g of pollen sample treated with 10 mL of $Ca(OH)_2$ and 10 mL of H_3PO_4 solutions (Figure 18). For this process, smaller amounts were used (1/8 ratio) instead of the amounts specified in the article. Similarly, instead of the 50 grams of pollen sample specified in the article, 6.25 grams of pollen sample was weighed and incubated with 25 mL of ethyl ether at room temperature overnight. SEM analysis confirmed the formation of well-defined calcium phosphate precipitates (Figure 17). At the same time, the amount of product obtained was higher for this method than for methods A and B.

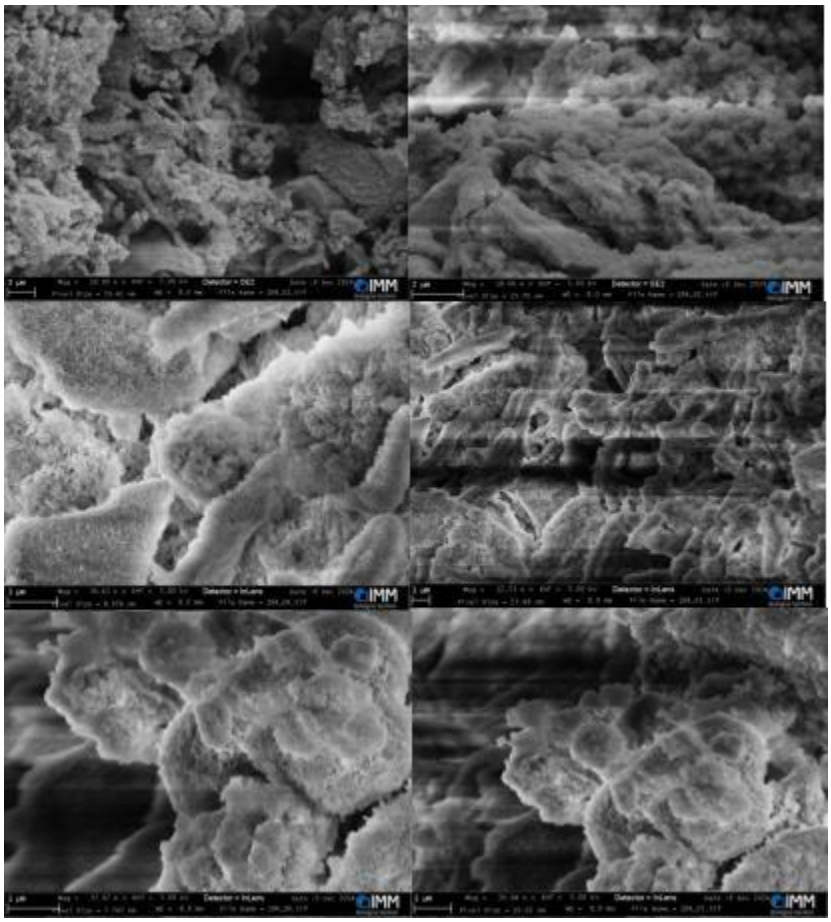

Figure 16. SEM images of Hydroxyapatite (produced by Method C)

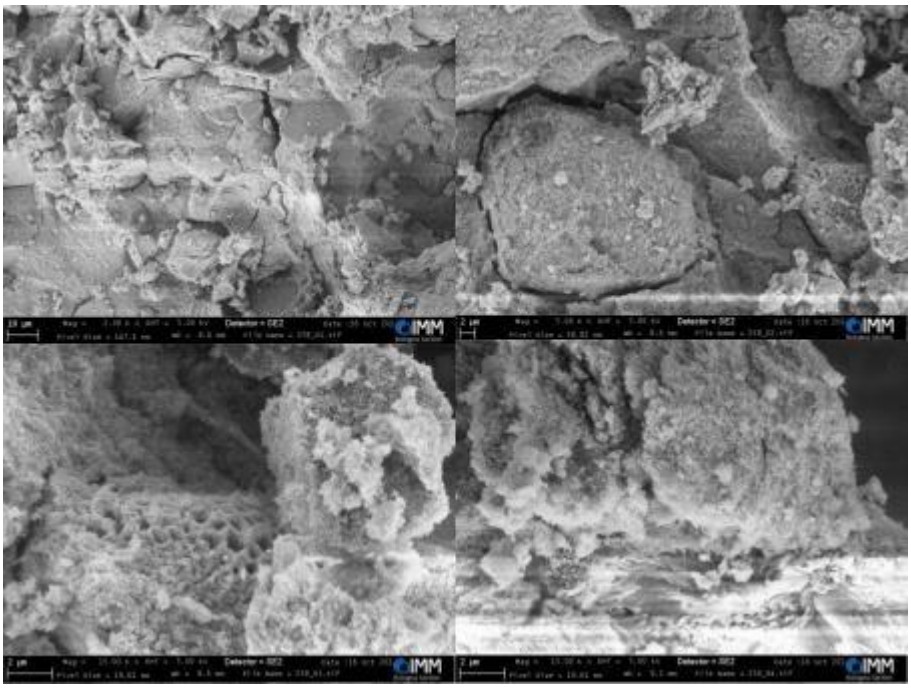

Figure 17. SEM images of Hydroxyapatite-exine complex produced by 50 mL 0.5 M of $Ca(OH)_2$ and 50 mL 0.03 M H_3PO_4

SEM images of empty exine capsules treated with hydroxyapatite obtained using method A showed successful HA formation inside the pollen shells, with external crystallization observed in some cases due to excessive precursor volume or concentration (Figure 18).

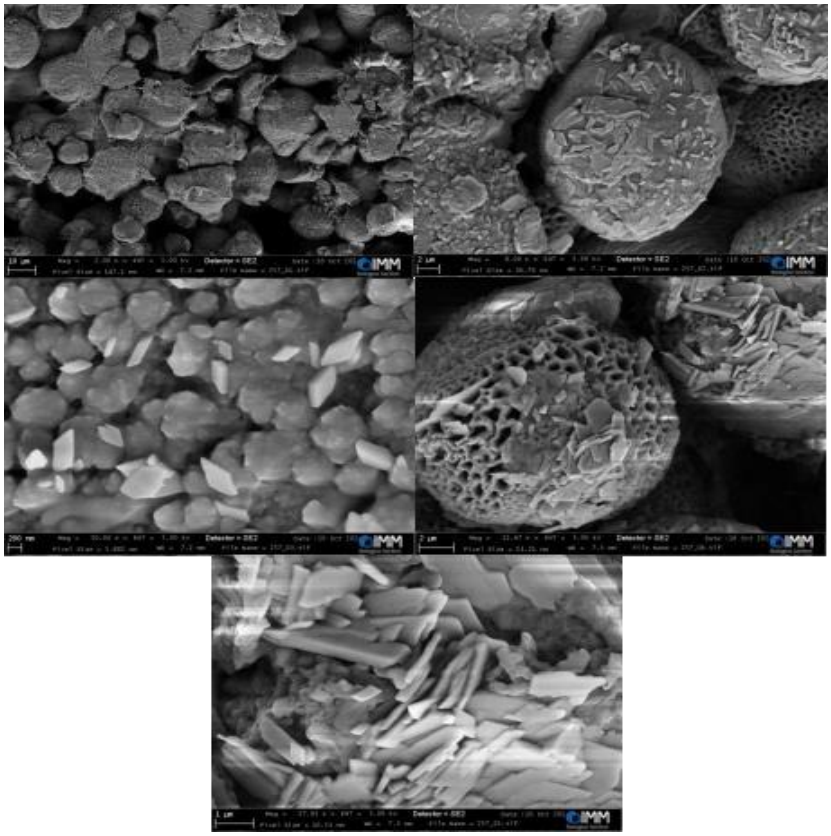

Figure 18. SEM images of Hydroxyapatite-exine complex produced by 10 mL 0.5 M of $Ca(OH)_2$ and 10 mL 0.03 M H_3PO_4

These observations provided information for further optimization aimed at maximizing intragranular filling while minimizing external accumulation. After discussions with the supervisor and calculations were completed, the same process was repeated using lower amounts of $Ca(OH)_2$ and H_3PO_4 .

As a result of the process, it was determined that the empty exine capsules could be successfully filled with hydroxyapatite, but the external accumulation decreased (Figure 19).

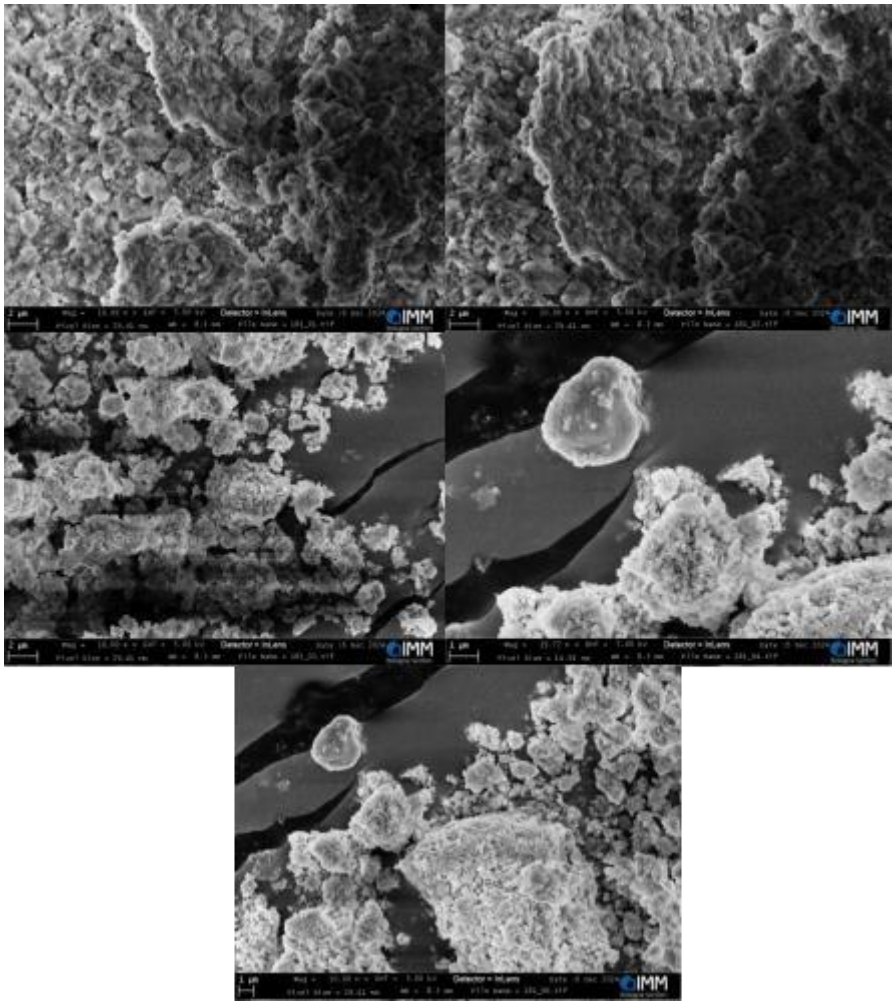

Figure 19. SEM images of Hydroxyapatite-exine complex produced by using Method C for HA

When examining the SEM images of the empty exine capsules processed with hydroxyapatite obtained using the C method, it was observed that the exine capsules were completely covered with hydroxyapatite, but due to the density of the hydroxyapatite crystals, it was observed that the exine capsules were completely covered. For this reason, the materials used in HA production were prepared at a 1:5 ratio, and the amount of empty exin capsules was doubled (0.4 g) to create a hybrid product. The method was repeated under the same conditions. The 1:5 ratio was maintained for yield analysis and calculation, and the method was repeated solely for hydroxyapatite production.

When SEM images were examined after two different processes were repeated under controlled conditions at 37°C and pH= 10 using the C method, it was observed that the exine capsules became more visible and the hybridization process with hydroxyapatite was successfully completed. Using Method C, two different processes were repeated under controlled conditions at 37°C and pH= 10, resulting in 0.950 grams of hydroxyapatite compound (opaque and white in color) and 1.251 grams of hybrid complex (opaque and beige in color).

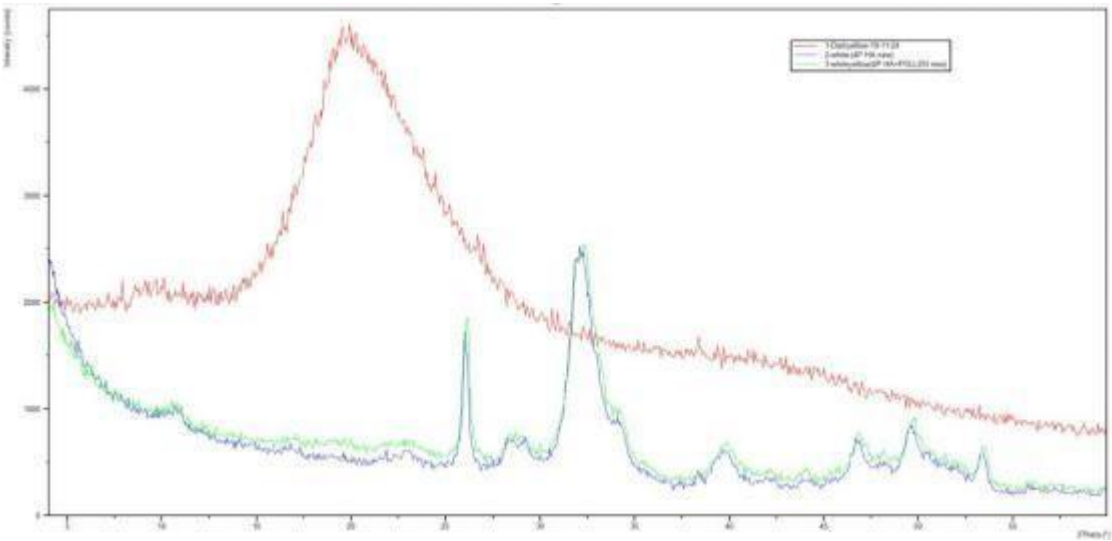

Figure 20. XRD results of: A)Raw pollen grains-red line B) Hydroxyapatite produced by method C, green line and C) Complex strucutre produced by HA (method C) + exine capsules(ethyl ether-assisted treatment), black line.

7. Applications in Dye and Pollutant Adsorptions

The dyes selected in this study to test the effectiveness of the composite material are substances commonly used to color materials such as silk, wool, cotton, and paper. While AR6 has an anionic (negatively charged) structure, MB (Methylene Blue) exhibits cationic (positively charged) properties. The MB molecule is particularly noteworthy because it has various applications in the medical field. It is known to be beneficial in the treatment of certain diseases such as anemia, malaria, and Barrett's esophagus. First produced as the first synthetic drug in the late 1800s, MB has since been used in various tests and treatments for human and animal health. Additionally, it enhances the effectiveness of chloroquine, a drug used in malaria treatment.

However, due to its widespread use in the textile industry, MB dye is often discharged into water sources without proper treatment. This poses serious risks to both the environment and human health. MB is a compound that is difficult to break down in nature and possesses toxic and carcinogenic properties. Its excessive accumulation not only degrades water quality and appearance but can also harm aquatic life and humans. Therefore, it is of great importance to treat wastewater containing MB using appropriate methods before discharging it into the environment. Today, various physical, chemical, and biological methods have been developed for the removal of such dyes.

Following these studies, the successfully produced Hydroxyapatite-Pollen capsule complex was used for adsorption tests for the removal of dyes and pollutants in accordance with the objective of the thesis.

7.1. Removal of Acid Red 6 Dye

The calibration curve for acid red dye (Figure 21) was constructed using different concentrations of the dye, ranging from 12ppm to 20ppm.

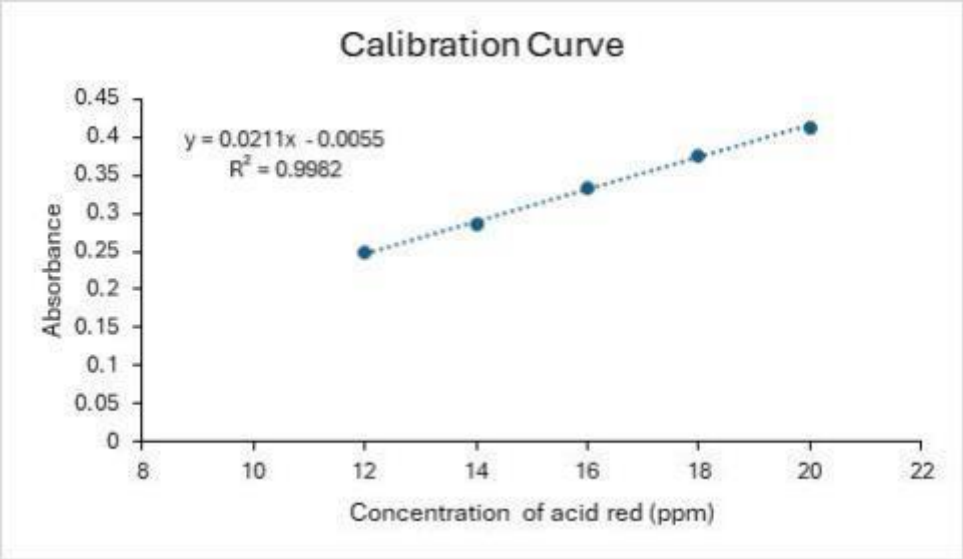

Figure 21. Calibration curve for AR6

Removal of AR6 from water was performed as reported in the experimental part. In Figure 22 are reported adsorption spectra obtained in the range 400-800 nm.

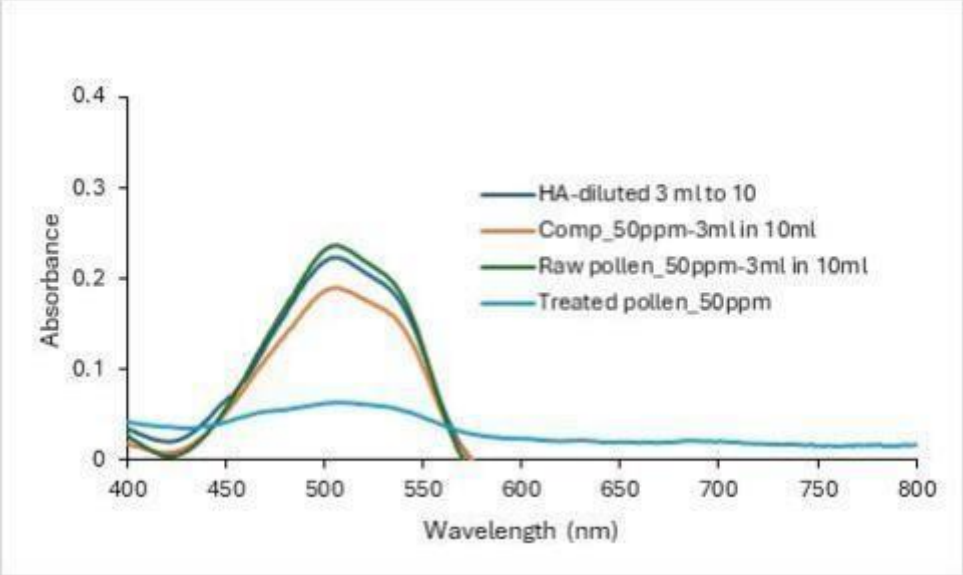

Figure 22. Absorption spectra of AR6 solution after contact with absorbent materials.

The results, reported in Table 1, indicated that the treated pollen effectively removed acid red dye, achieving a removal efficiency of 93.45%, likely due to its high surface area. In contrast, the composite material exhibited a lower removal efficiency of 38.22%, possibly due to the saturation of the pollen surface with hydroxyapatite, which may have hindered dye interaction. Additionally, the raw pollen showed the lowest removal efficiency (23.70), which could be attributed to its natural waxy

coating, limited surface area, lack of active functional groups, and suboptimal surface charge, which restrict its ability to adsorb or interact effectively with dye molecules.

Adsorbents	abs	dil. Ce (ppm)	Ce (ppm)	Co (ppm)	RE (%)	Qe (mg/g)
Raw pollen	0.24	11.44	38.15	50.00	23.70	14.81
Treated pollen	0.06	3.28	3.28	50.00	93.45	58.40
HA	0.22	10.90	36.33	50.00	27.33	17.08
Composite	0.19	9.27	30.89	50.00	38.22	23.89

Table 1. Removal efficiency and adsorption capacity of different materials on AR6.

7.1.1. Effect of pH On Adsorption of Acid Red

The experiment was conducted by treating 25 mL of a 50ppm acid red dye solution with 20 mg of adsorbents for 2 hours at a temperature range of 26–30 ºC and a stirring speed of 300 rpm. The effect of pH on dye removal was evaluated within a neutral to basic pH range. Collected spectra are reported in Figure 23. The highest removal efficiency (Table 2) was observed around neutral pH (pH 7) for both adsorbents. The results, depicted in Figure 22, showed a decline in removal efficiency with increasing pH for both the composite material and treated pollen. This decrease at higher pH levels can be attributed to the increased concentration of hydroxide ions in the solution, which compete with the negatively charged dye molecules for adsorption sites, thereby reducing adsorption efficiency (Wang et al., 2020).

Adsorbent	pH	Abs	dil. Ce (ppm) (1 in 2)	Ce (ppm)	Co (ppm)	RE (%)	Qe (mg/g)
Composite	10.07	0.44	21.19	42.38	50.00	15.23	9.52
	9.16	0.42	20.35	40.71	50.00	18.58	11.62
	8.18	0.41	19.46	38.91	50.00	22.18	13.86
	7.16	0.37	17.79	35.58	50.00	28.84	18.02
Treated Pollen	10.06	0.49	23.66	47.33	50.00	5.34	3.34
	9.05	0.44	21.10	42.20	50.00	15.59	9.74
	8.03	0.45	21.48	42.96	50.00	14.08	8.80
	7.01	0.43	20.74	41.47	50.00	17.05	10.66

Table 2. Effect of pH on adsorption of AR6

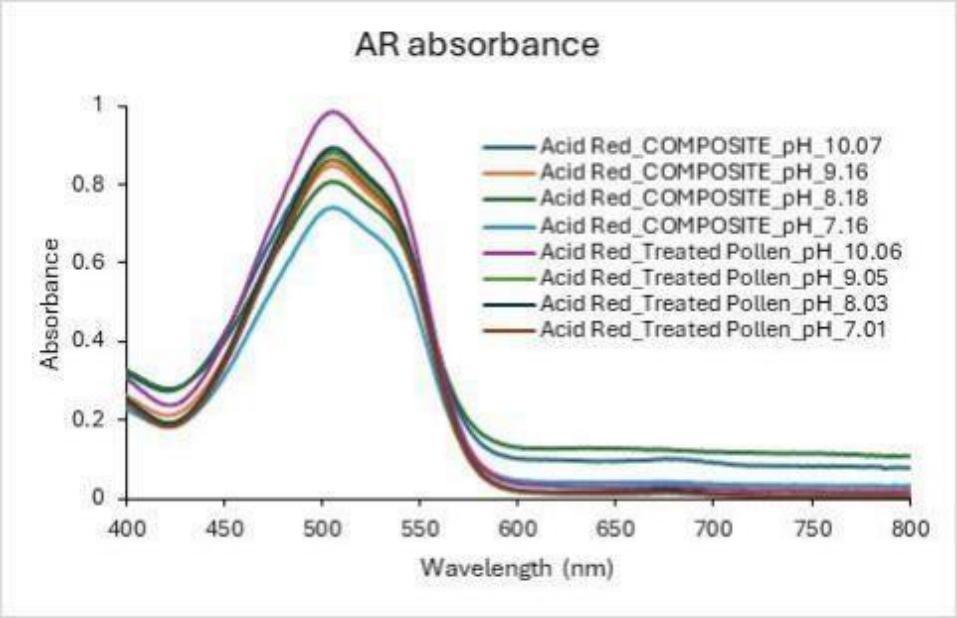

Figure 23. AR6 spectra after adsorption on composite material and treated pollen as a function of pH.

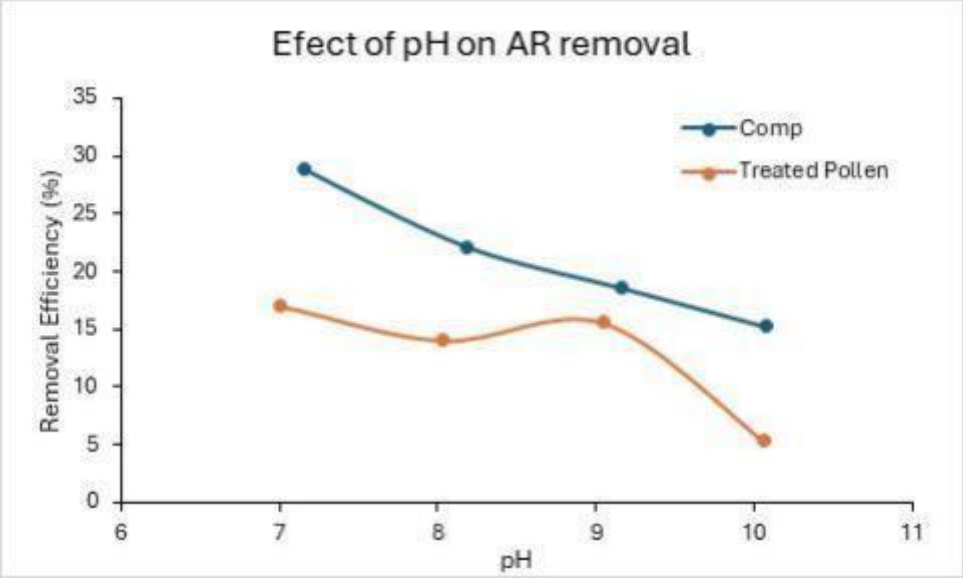

Figure 24. Correlation between pH and RE% for AR6

7.2. Removal of Methylene Blue Dye

The calibration curve for methyl blue dye, reported in Figure 25, was developed by measuring the absorbance of methyl blue solution with 1-5ppm.

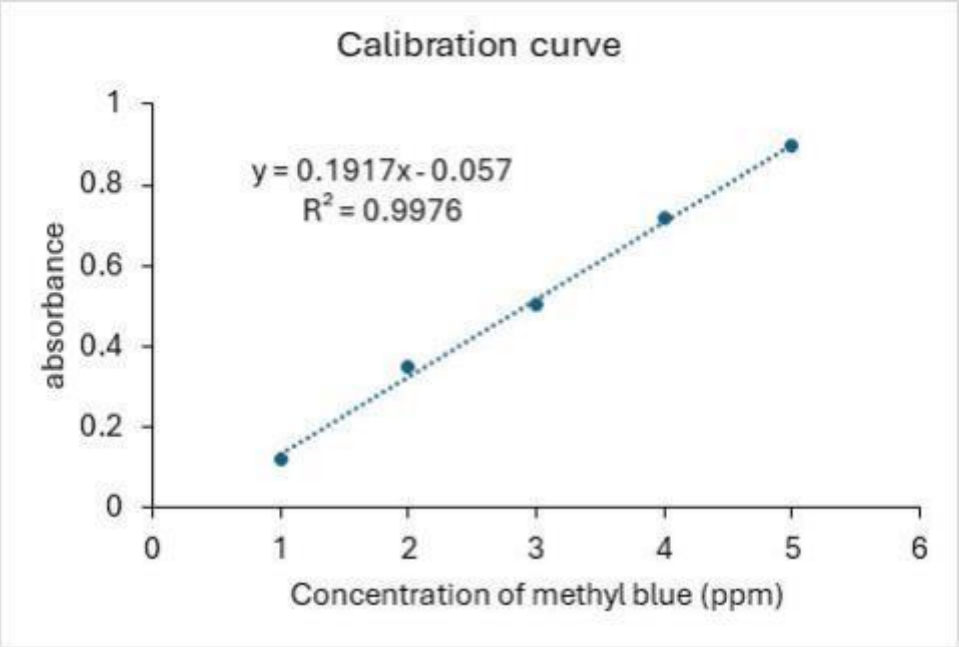

Figure 25. Calibration curve ofMB

Removal of MB from water was performed as reported in the experimental part. In Figure 26 are reported absorption spectra obtained in the range 400-800 nm.

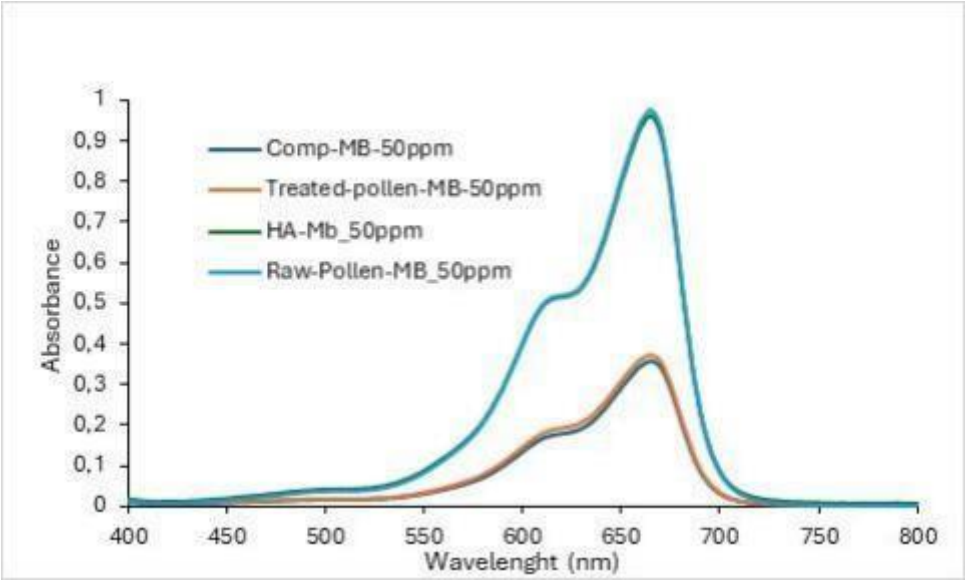

Figure 26. Absorption spectra of MB solution after contact with absorbent materials.

Removal efficiency and adsorption capacity of different materials are reported in Table 3.

The results indicated that both the composite material and treated pollen effectively removed methylene blue, achieving removal efficiencies of 63.92% and 62.75%, respectively. This enhanced performance can be attributed to their higher surface area,

which facilitated greater adsorption of methylene blue molecules. In contrast, untreated pollen and hydroxyapatite exhibited minimal removal efficiency.

Adsorbent	abs	dil. Ce (ppm)	Ce (ppm)	Co (ppm)	RE (%)	Qe (mg/g)
Raw pollen	0.98	5.40	54.05	60.00	9.92	7.44
Treated pollen	0.37	2.23	22.35	60.00	62.75	47.06
HA	0.96	5.33	53.31	60.00	11.15	8.36
Composite	0.36	2.16	21.65	60.00	63.92	47.94

Table 3. Removal efficiency and adsorption capacity of different materials on MB.

7.2.2. Effect of pH on Removal of MB

The effect of pH on removal of methyl blue was examined by treating 25ml of 50ppm methyl blue dye solution with 20mg of adsorbent (composite material or treated pollen) at different pH ranging from neutral to basic (7-10). Figure 27 reported the spectra collected at different pH.

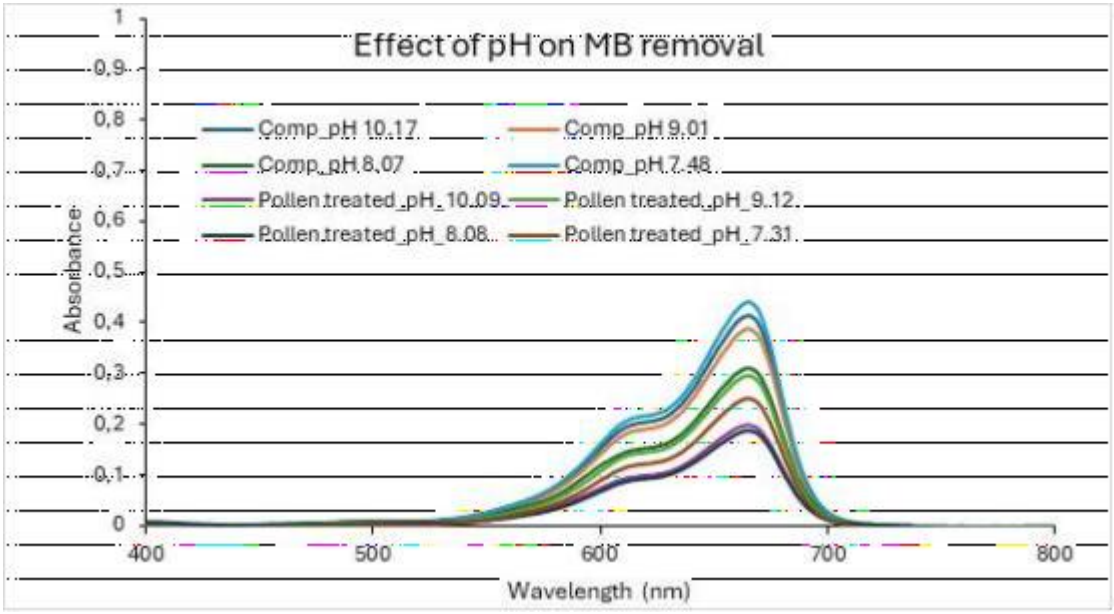

Figure 27. MB spectra after adsorption on composite material and treated pollen as a function of pH.

The results revealed that treated pollen consistently showed higher removal efficiency, peaking at 74.44% at pH 8.08, while the composite material reached a maximum of 61.70% at pH 8.07. Both

adsorbents performed best around pH 8, with a slight decline beyond this, likely due to competition between hydroxide ions and MB molecules for adsorption sites. The superior performance of treated pollen is attributed to its enhanced surface area and functional groups, while the performance of the composite material decreased at higher pH, likely due to saturation of available adsorption sites. These findings highlight that neutral to slightly basic conditions are optimal for MB removal. This finding aligns with previous studies that reported maximum removal efficiency of methyl blue dye at pH 8 (Pathania et al., 2017, Hua et al., 2023). However, another study has suggested that the removal of cationic dyes, such as methyl blue, could increase with rising pH due to the electrostatic attraction between the cationic dye and the negatively charged surface of the adsorbents (Paluch et al., 2023).

Adsorbent	pH	Abs	10*dil.Ce (ppm)	Ce (ppm)	Co(ppm)	RE (%)	Qe (mg/g)
Composite	10.1 7	0.41	2.45	24.52	50.00	50.95	31.85
	9.01	0.39	2.32	23.22	50.00	53.57	33.48
	8.07	0.31	1.92	19.15	50.00	61.70	38.56
	7.48	0.44	2.59	25.90	50.00	48.20	30.13
Treated Pollen	10.0 9	0.20	1.34	13.39	50.00	73.22	45.76
	9.12	0.29	1.83	18.33	50.00	63.35	39.59
	8.08	0.19	1.28	12.78	50.00	74.44	46.52
	7.31	0.25	1.60	16.01	50.00	67.99	42.49

Table 4. Removal efficiency and adsorption capacity of Composite product and exine capsules(treated) on MB.

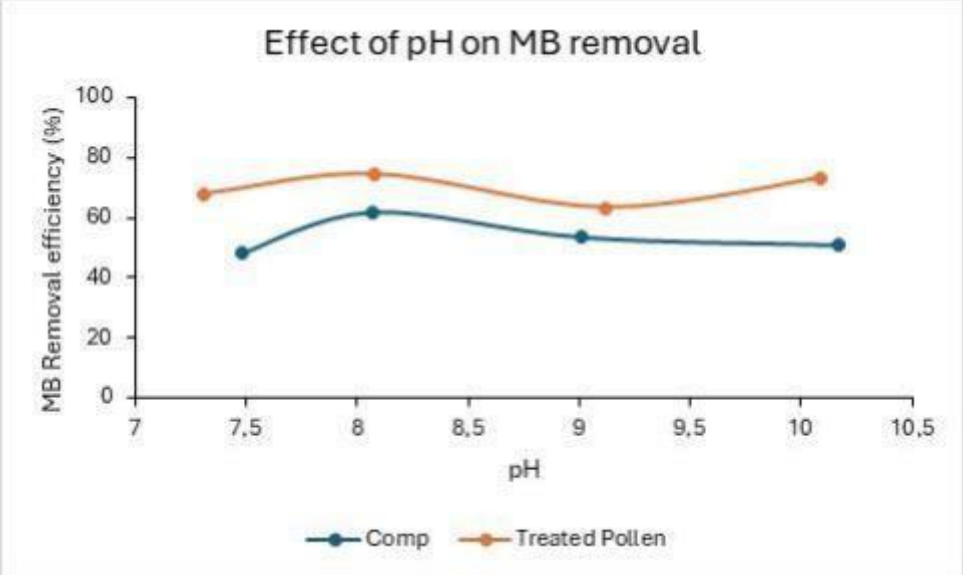

Figure 28. Correlation between pH and RE% A)for MB removal by complex product and B)for MB removal by exine capsules

8. Pb2+ Removal From Water

Following the article of "Effective adsorption and removal of malachite green and Pb2+ from aqueous samples and fruit juices by pollen–inspired magnetic hydroxyapatite nanoparticles/hydrogel beads(Hua, Y. et al, 2023), adsorption experiments were performed on HA to investigate properties. The adsorption conditions were assessed as a function of pH: as HA is soluble at acidic pH, the adsorption efficiency was assessed in the range 6- 12. The pH was adjusted by NaOH (1 mol/L) and measured by pH meter. 20 mg of adsorbent were soaked in 20 ml of 10 mM solution of Pb(NO3)2 at room temperature and kept under stirring at 300 rpm for 2 hours. The suspension was centrifuged at 10000 rpm for 5 minutes and the Pb2+ concentration was measured using ICP-MS.

A calibration curve was previously obtained in the range 5-50ppm and reported in Figure 29.

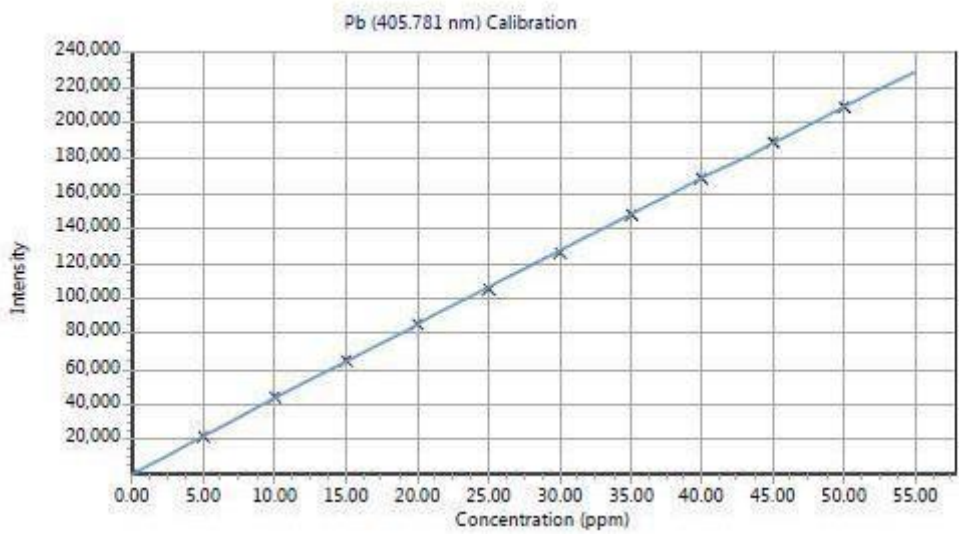

Figure 29. Calibration curve of Pb2+

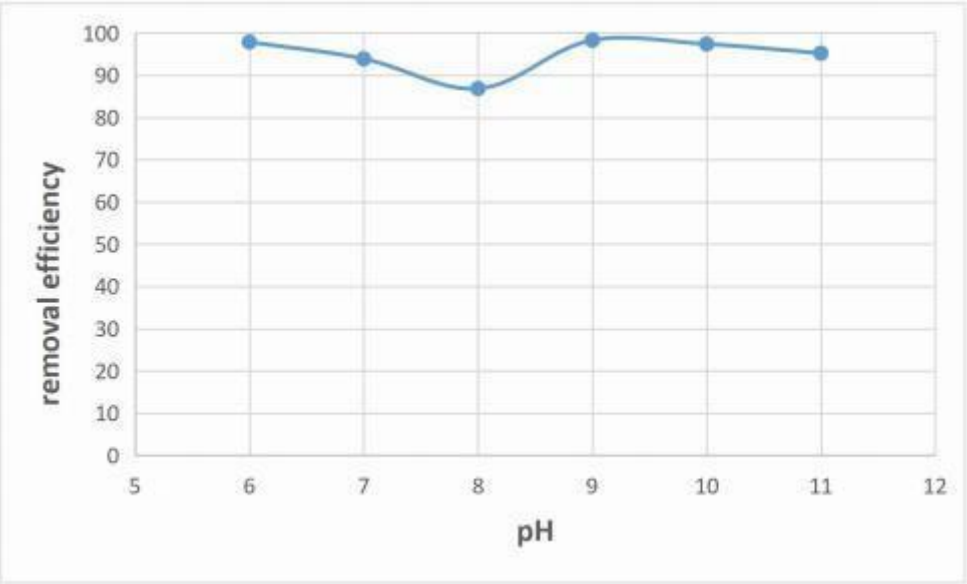

Figure 30. The Pb2+ removal efficiency by using HA

9. Conclusions

In this thesis study, the biomaterial potential of pollen grains, which are abundant in nature and play important roles in plant pollination, was investigated. In particular, the feasibility of using exin - based capsules with hollowed-out internal structures, functionalized with hydroxyapatite (HA), in both biomedical and environmental applications was explored. In this context, different pollen types were analyzed, and Millefiori pollen was determined to be the most suitable structural form, which was preferred in experimental applications.

As a result of the chemical pretreatments applied to the pollen grains, the pollen content was successfully removed, and hollow exine structures with preserved external morphology were obtained. A comparative evaluation was conducted using three different methods: Method A (pure alkaline), Method B (pure acidic), and Method C (ether-assisted acidic treatment). The results showed that Method C, in particular, significantly removed organic residues, activated functional groups (carboxyl, hydroxyl, etc.) on the surface, and provided high porosity.

These exine structures were then converted into hybrid composites via in-situ hydroxyapatite synthesis. Testing different reactive volumes during the precipitation process significantly affected the distribution of HA between the capsule interior and exterior surface. In synthesis using low reactive volumes, it was observed that HA integrated more controllably into the pollen interior surface, minimizing external precipitation. These structures were characterized by SEM analysis; HA crystals were found to be nano-sized, irregular, and plate-like in morphology. It was

understood that these crystals were homogeneously distributed on the pollen surface and were in chemical interaction with the exine layer.

The potential of the composites for environmental applications was tested with pollutants such as methylene blue, acid Red 6 and Pb^2 ions. The results obtained showed that HA-supported exine capsules have a high retention capacity through both physical adsorption (via pores) and chemical binding (ion exchange and complexation). The solubility of HA increases at acidic pH (lower than 5) and allows this composite material to work in a pH range from 6 to 11. These range of pH is consistent whit the pH of waste water.
This opens the door to the development of targeted, smart sorption systems for wastewater treatment.
Additionally, BCA protein analysis revealed that protein residues were eliminated by 60% in pollen processed using Method C, suggesting that the capsules could be used as biocompatible carrier systems. This means that pollen-based structures could be evaluated not only in environmental applications but also in biomedical fields such as drug delivery, tissue regeneration, and biosensor platforms.

The data obtained in this thesis contributes to the literature by demonstrating how natural biomaterials can be functionalized in sustainable technologies. These pollen-based systems are not only inexpensive and abundant biological resources but also attract attention due to their susceptibility to versatile chemical modifications. By offering environmentally friendly, energy-efficient, and high-performance alternatives compared to traditional synthetic materials, they could occupy a leading position in green engineering and functional material development studies.

In conclusion, pollen-based hydroxyapatite composites form a powerful platform that can be at the center of multidisciplinary research and applications, both as naturally sourced adsorbent systems and as functional biocomposites. This study once again highlights the immense potential of biomaterials inspired by nature for the sustainable and smart material technologies of the future.

10. References

- Ariizumi, T., & Toriyama, K. (2011). Genetic regulation of sporopollenin synthesis and pollen exine development. Annual Review of Plant Biology, 62, 437 – 460. https://doi.org/10.1146/annurev-arplant-042809-112312

-Domínguez, E., Mercado, J. A., Quesada, M. A., & Heredia, A. (1999). Pollen sporopollenin: Degradation and structural elucidation.Sexual Plant Reproduction, 12(3), 171–178.https://doi.org/10.1007/s004970050189

-Edlund, A. F., Swanson, R., & Preuss, D. (2004). Pollen and stigma structure and function: The role of diversity in pollination. The Plant Cell, 16(Suppl. 1), S84–S97. https://doi.org/10.1105/tpc.015800

-Lee, H., Dellatore, S.M., Miller, W.M., & Messersmith, P.B. (2007). Mussel=inspired surface chemistry for multifunctional coatings. Science, 318(5849), 426–430. https://doi.org/10.1126/science.11 47241

-Luo, Y., Sun, Y., & Zhu, J. (2021). Pollen-derived functional materials: Natural templates for advanced applications. ACS Sustainable Chemistry & Engineering, 9(5), 2023–2036. https://doi.org/10. 1021/acssuschemeng.0c08529

-Mohan, D., Pittman Jr., C. U., & Steele, P. H. (2020). Sustainable biosorbents and their applications in water remediation: A review. Bioresource Technology, 324, 124630. https://doi.org/10.1016/j.biortech.2020.124630

-Piffanelli, P., Ross, J. H. E., & Murphy, D. J. (1998). Biogenesis and function of the lipidic structures of pollen grains. Sexual Plant Reproduction, 11(2), 65–80. https://doi.org/10.1007/s004970050125

-Scott, R. J., Spielman, M., & Dickinson, H. G. (2004). Stamen structure and function. The Plant Cell, 16(Suppl_1), S46–S60. https://doi.org/10.1105/tpc.017020

-Chen, X., Li, Y., Wang, Z., Liu, J., & Huang, Y. (2021). Composite adsorbents of hydroxyapatite and biomass: A green approach for heavy metal removal. Environmental Research, 195, 110856. https://doi.org/10.1016/j.envres.2021.110856

-Huang, W., Zhou, M., & Zhang, H. (2021). Functionalized pollen grains for efficient removal of dyes and metals from wastewater. Chemical Engineering Journal, 426, 131885. https://doi.org/10.1016/j.cej.2021.131885

-Kim, H. M., Himeno, T., Kawashita, M., & Kokubo, T. (2013). Novel bioactive materials with high surface reactivity: Hydroxyapatite with controlled ion substitution. Journal of the American Ceramic Society, 96(2), 330–336. https://doi.org/10.1111/jace.12132

-Liu, J., Zhang, H., Chen, Y., & Wang, Y. (2020). Biomass-derived functional materials for environmental remediation. Bioresource Technology, 302, 122854. https://doi.org/10.1016/j.biortech.2020.122854

-Mondal, S., Pal, S., & Roy, T. (2019). Waste-derived hydroxyapatite: Synthesis, characterization and application in environmental remediation. Materials Science and Engineering: C, 100, 623–636. https:// doi.org/10.1016/j.msec.2019.03.045

-Wang, L., Nancollas, G. H., & Grynpas, M. D. (2006). Dissolution behavior of hydroxyapatite in acidic conditions: Effects of pH and ionic strength. Journal of Dental Research, 85(2), 134–138. https://doi.org/10.1177/154405910608500209

-Zhou, C., Wu, Y., Chen, X., & Zhang, D. (2022). Efficient removal of heavy metals using modified natural pollen: A sustainable biosorbent. Journal of Hazardous Materials, 421, 126739. https://doi.org/10.1016/j.jhazmat.2021.126739

-Kingston, R. E., Chen, C. A., & Okayama, H. (2001). Calcium phosphate transfection. In Current Protocols in Immunology (Appendix 1C). John Wiley & Sons.

-Yang, Y., Mou, Z., Liu, Q., Wang, B., Luo, C., Xu, Y., Huang, Q., He, B., Chang, K., Wang, G., You , Z., & Qian, H. (2024). Sunflower pollen-derived microspheres selectively absorb DNA for microRNA detection. Chembiochem: A European Journal of Chemical Biology, 25(20), e202400249. https://doi.org/10.1002/cbic.202400249

-Guo, G., Wang, Y., & Guo, H. (2004). Study on the synthesis of hydroxyapatite nanoparticles by the chemical precipitation method. Journal of Materials Science: Materials in Medicine, 15(3), 229–234.

-Tas, A. C. (2000). Synthesis of biomimetic calcium hydroxyapatite powders at 37°C in synthetic body fluids. Biomaterials, 21(14), 1429–1438. https://doi.org/10.1016/S0142-9612(00)00019-3

-Hua, Y., Xu, D., Liu, Z., Zhou, J., Han, J., Lin, Z., Xu, D., Chen, G., Huang, X., Chen, J., Lv, J., & Liu, G. (2023). Effective adsorption and removal of malachite green and Pb^2 from aqueous samples and fruit juices by pollen-inspired magnetic hydroxyapatite nanoparticles/hydrogel beads. Journal of Cleaner Production, 411, 137233.

-Paluch, D., Bazan-Wozniak, A., Nosal-Wiercińska, A., & Pietrzak, R. (2023). Removal of methylene blue and methyl red from aqueous solutions using activated carbons obtained by chemical activation of caraway seed. Molecules.

-Pathania, D., Sharma, S., & Singh, P. (2017). Removal of methylene blue by adsorption onto activated carbon developed from Ficus carica bast. Arabian Journal of Chemistry, 10, S1445–S1451.

-Wang, Q., Liang, L., Xi, F., Tian, G., Mao, Q., & Meng, X. (2020). Adsorption of azo dye Acid Red 73 onto rice wine lees: Adsorption kinetics and isotherms. Advances in Materials Science and Engineering, 2020, 3469579.

-Hua, Y., Xu, D., Liu, Z., Zhou, J., Han, J., Lin, Z., Xu, D., Chen, G., Huang, X., Chen, J., Lv, J., Liu, G., & Zhao, Y. (2023). Effective adsorption and removal of malachite green and Pb^2 from aqueous samples and fruit juices by pollen-inspired magnetic hydroxyapatite nanoparticles/hydrogel beads. Journal of Cleaner Production, 411, Article 137233. https://doi.org/10.1016/j.jclepro.2023.137233

-De Mori, A., Quizon, D., Dalton, H., Yavuzyegit, B., Cerri, G., Antonijevic, M., & Roldo, M. (2024). Sporopollenin capsules as biomimetic templates for the synthesis of hydroxyapatite and β-TCP. Biom imetics, 9(3), 159. https://doi.org/10.3390/biomimetics9030159

Acknowlegments

I would like to express my gratitude to my very valuable Professor Prof.essa Silvia Panzavolta for being there for me at every moment and in every difficulty, with all her empathy and support. She never withheld her knowledge and skills from me and made me feel very lucky throughout the process. I am very happy that I had the opportunity to work with her. I wish I could have focused only on my lessons instead of my responsibilities related to my life flow and benefited more from her wealth of knowledge.

I would like to thank and remember with great longing my beautiful mother pek Erdem, who has always been there for me throughout my life, who has always inspired me with her strength and has been my idol, my dear brother Bora Erdem, who shines like a diamond and always supports me with his energy, my sister Dilara Erdem, whose little sister I am proud to be, and the best father in the world , Enver Erdem, who I know is watching me proudly from the most beautiful corner of heaven.

Even though he is not with us now.